Estuarine, Coastal and Shelf Science 275 (2022) 107997

Contents lists available at ScienceDirect

Estuarine, Coastal and Shelf Science

journal homepage: www.elsevier.com/locate/ecss

Changes in the burial efficiency and composition of terrestrial organic carbon along the Mackenzie Trough in the Beaufort Sea

Dahae Kim [a,b], Jung-Hyun Kim [a,*], Tommaso Tesi [c], Sujin Kang [b], Alessio Nogarotto [c], Kwangkyu Park [a], Dong-Hun Lee [b,1], Young Keun Jin [a], Kyung-Hoon Shin [b], Seung-Il Nam [a]

[a] Korea Polar Research Institute, 26 Songdomirae-ro, Yeonsu-gu, Incheon, 21990, South Korea
[b] Department of Marine Science and Convergence Technology, Hanyang University ERICA Campus, 55 Hanyangdaehak-ro, Sangnok-gu, Ansan-si, Gyeonggi-do, 15588, South Korea
[c] Institute of Marine Sciences, National Research Council (ISMAR-CNR), Bologna, Italy

ARTICLE INFO

Keywords:
Beaufort sea
Mackenzie trough
Terrestrial organic carbon
$\delta^{13}C$
$\Delta^{14}C$
n-alkanes
Lignin phenols

ABSTRACT

In this study, we investigated surface sediments collected along a Mackenzie Trough transect during the R/V Araon expeditions (ARA04C, ARA05C, and ARA08C) in the Beaufort Sea in 2013, 2014, and 2017. We applied various inorganic and organic geochemical tools (major elements, carbon and nitrogen contents, stable carbon and radiocarbon isotope compositions, and molecular biomarkers) in combination with sedimentological measurements (mineral surface area (SA) and grain size) to assess the source and burial characteristics of organic carbon (OC). In general, the sediment mean grain size decreased with water depth whereas the SA increased, resulting in a decrease in the OC loading and the burial efficiency of terrestrial OC. The sedimentary OC was further influenced by the loss of terrestrial OC and replacement with marine OC with increasing water depth. Accordingly, our results suggest that hydrodynamic sorting and degradation of terrestrial OC co-occurred together with the enrichment of marine OC with distance offshore. Such processes controlled the burial and reactivity of terrestrial OC along the Mackenzie Trough transect.

1. Introduction

Permafrost regions cover approximately a quarter of the Northern Hemisphere land surface (Zhang et al., 1999) and contain ~1300 Pg of soil OC (Hugelius et al., 2014); this exceeds the current atmospheric carbon pool (860 Pg, Friedlingstein et al., 2019) and is equivalent to ~40% of the global soil OC (Tarnocai et al., 2009). Recent amplified Arctic warming is twice as fast as the global average (IPCC et al., 2013); this has caused significant permafrost thawing, leading to growing concerns for potential positive permafrost carbon–climate feedbacks (Schurr et al., 2015; Grosse et al., 2016). Ongoing climate change is predicted to increase the Arctic permafrost thaw-release of soil OC to the Arctic Ocean via river discharge and coastal erosion (Gustafsson et al., 2011; Barnhart et al., 2014; Haine et al., 2015). Following permafrost release, aged OC is either buried in coastal sediments, transported to deeper basins, or degraded to greenhouse gases such as CO_2 (Stein and MacDonald, 2004; Sánchez-García et al., 2011; Semiletov et al., 2016). Therefore, it is essential to understand the ultimate fate of thawed permafrost OC in marine environments to better predict future Arctic carbon cycles and climate change (Vonk and Gustafsson, 2013).

In the Canadian Beaufort Sea, the Mackenzie Shelf (area of 64,000 km^2 and length of 150 km) extends from the coastal lowlands of the Yukon and Northwest Territories of Canada to the shelf break at approximately 80 m water depth (Shearer, 1971). The shelf represents less than 2% of the Arctic Ocean's total shelf area (Stein and MacDonald, 2004). The Mackenzie Trough borders the Mackenzie Shelf to the west and the Amundsen Gulf to the east. The Mackenzie River delivers suspended particles to the Mackenzie Shelf, is the largest Arctic river in terms of sediment discharge (~127 × 10^6 t/yr; Stein and MacDonald, 2004), and the fourth largest in terms of freshwater discharge (~306 ± 10 km^3/yr; McClelland, 2016). The Mackenzie River is therefore the largest single source of sediments to the Arctic Ocean that even exceeds the total sediment discharge of all other Arctic rivers combined (Stein and MacDonald, 2004; O'brien et al., 2006). Moreover, the Mackenzie River is the primary source (95%) of particulate terrestrial organic matter to the Mackenzie Shelf (Macdonald et al., 1998). The Mackenzie

* Corresponding author.
E-mail address: jhkim123@kopri.re.kr (J.-H. Kim).
[1] Present address: National Institute of Fisheries Science, 216 Gijanghaean-ro, Gijang-eup, Gijang-gun, Busan 26083, South Korea.

https://doi.org/10.1016/j.ecss.2022.107997
Received 29 July 2021; Received in revised form 11 July 2022; Accepted 18 July 2022
Available online 21 July 2022

Trough is a 75-km-wide, ~130-km-long glacial cross-shelf valley (Rampton, 1982) and is an important conduit for the export of suspended particles (via the Mackenzie River) and the deposition of sediments in the Canada Basin (Blasco et al., 1990; Carmack and Macdonald, 2002). Thawing permafrost in a warming Arctic is expected to amplify the delivery of terrestrial OC to the Arctic shelves (e.g., Mann et al., 2022). Thus, knowledge about the fate of terrestrial OC during cross-shelf transport is a key to understand to what extent permafrost-derived OC would be sequestered in marine sediments, regulating the atmospheric CO_2 levels on geological timescales (e.g., Eglinton et al., 2021).

Previous studies in the Canadian Beaufort Sea have investigated the origin of sedimentary OC in the Mackenzie Shelf using sediment bulk characteristics, including the total nitrogen to total organic carbon ratio (N_{tot}/TOC), and the stable carbon and radiocarbon isotope compositions (e.g., Macdonald et al., 1998; Naidu et al., 2000; Goñi et al., 2000, 2005, 2013; Magen et al., 2010; Vonk et al., 2015). Other studies have investigated surface sediments at the molecular level, including *n*-alkanes, sterols, and lignin phenols (Yunker et al., 1995, 2005; Goñi et al., 2000, 2005, 2013; Belika et al., 2004; Drenzek et al., 2007). High molecular weight (HMW) *n*-alkanes are derived from vascular plant leaf waxes (Eglinton and Hamilton, 1967) and thus have been widely used as a terrestrial biomarker in the Arctic Ocean (e.g., Yunker et al., 1995, 2005). Sterols have been used as source markers of both higher plants and marine phytoplankton (e.g., Huang and Meinschein, 1976; Volkman, 1986). Lignins are common to all vascular plants (Hedges and Mann, 1979), whereas cutins are mainly associated with the soft tissues of vascular plants such as leaves and needles (e.g., Goñi and Hedges, 1995). Hence, both lignin phenols and cutin acids have been commonly used as terrestrial biomarkers in the Arctic Ocean (e.g., Goñi et al., 2000, 2013; Vonk et al., 2015). Overall, the previous studies using molecular biomarkers showed that terrestrial OC accounts for the majority (50–80%) of OC in shelf and slope surface sediments. However, most sediment samples in these studies were collected before 1987. Considering the abrupt climatic change in the Arctic over the last decades, these studies may not capture the recent pace of Canadian Arctic permafrost thawing, particularly as the Arctic is warming much faster than the global average.

In this study, we considered ten surface sediment samples collected during three expeditions of *R/V* Araon (ARA04C, ARA05C, and ARA08C) in the Beaufort Sea in 2013, 2014, and 2017 to investigate spatial variation in sedimentary OC composition along a transect in the Mackenzie Trough. For this purpose, we applied both bulk (SA, grain size, major elements, carbon and nitrogen contents, and stable and radioactive isotopic compositions) and molecular (*n*-alkanes, sterols, lignin phenols, and cutin acids) parameters. Our main objectives were 1) to investigate first-order controls on OC loading, 2) to constrain the source and degradation status of sedimentary OC, 3) to assess the burial efficiency of terrestrial OC, and 4) to discern the source contribution (biogenic and petrogenic OC) of sedimentary OC, by comparing our results with previously published data in the study area (Goñi et al., 2005, 2013; Drenzek et al., 2007; Magen et al., 2010; Hilton et al., 2015; Vonk et al., 2015). Our results from the Mackenzie Trough transect provide new insights into the burial and reactivity of terrestrial OC in the Canadian Beaufort Sea.

2. Materials and methods

2.1. Sample collection

We used a box corer and a multi-corer to collect surface sediment samples (0–1 cm; n = 10) along the Mackenzie Trough during three cruises on the Korean icebreaker *RV Araon* (ARA04C, ARA05C, and ARA08C) in the Canadian Beaufort Sea in 2013, 2014, and 2017 (Fig. 1, see also Table S1). The collected sediments generally consisted of olive-gray clayey silt. Once recovered, the cores were sliced at 1-cm intervals, placed in glass jars, stored frozen, and freeze-dried for further analyses.

2.2. Surface area analysis

Specific SA analyses were performed using a particle and pore size analysis system (NanoPlus, ASAP2420 AutoporeIV) at the Korea Basic Science Institute (KBSI, Jeonju Center). The freeze-dried, unground subsamples (~0.5 g) were desalted three times by mixing with 50 mL Milli-Q water, centrifugation (1 h at 30,000×*g*), and removal of supernatant water, followed by freeze-drying. To remove organic material, the freeze-dried samples were then heated to 350 °C for 12 h and then gently cooled to room temperature over 12 h. Prior to analysis, the dry samples were degassed at 200 °C for 2 h in a Micromeritics FlowPrep 060 Sample Degas System under a constant N_2 flow. Each analysis was

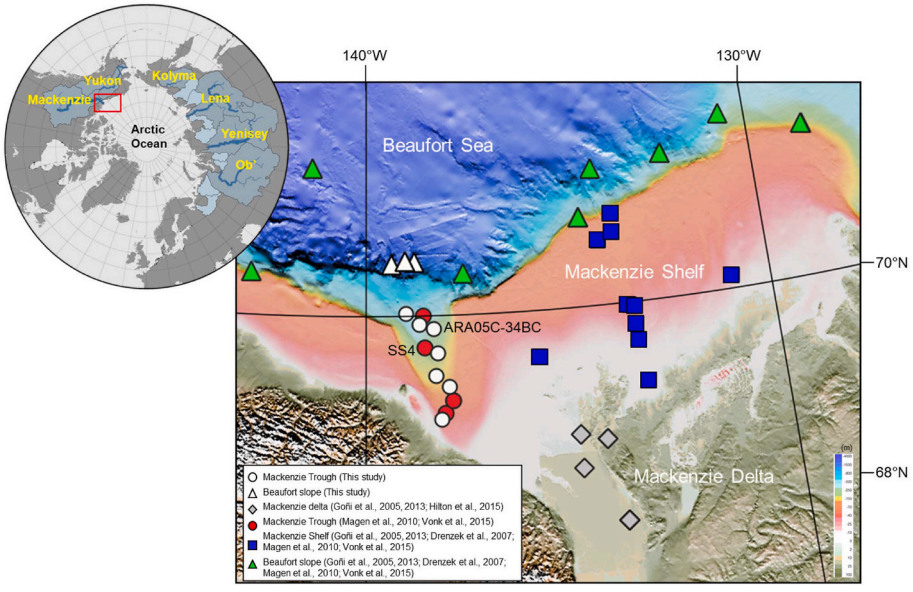

Fig. 1. Map of the study area in the Beaufort Sea showing major Arctic rivers flowing into the Arctic Ocean. Open circles mark the sampling sites in the Mackenzie Trough, and open triangles indicate the sites in the Beaufort slope. The sample locations from previous studies are also displayed with different colors and symbols. (For interpretation of the references to color in this figure legend, the reader is referred to the Web version of this article.)

initiated by measuring the free space in the vial. The specific SAs were measured using an N_2 gas adsorbate in a He atmosphere, with six pressure point measurements (relative pressure p/p0 = 0.05–0.3, equilibration time 5 s, following Mayer (1994)). The analytical precision was better than ±9%, and the instrument performance was monitored using the SA reference material Carbon Black (21.0 ± 0.75 m^2/g; ISO 9277:2010) provided by Micromeritics.

2.3. Grain size analysis

Grain size distribution was determined following the procedure previously reported by Joo et al. (2019). Briefly, an aliquot (~5 g) of the freeze-dried subsamples was treated with 5 mL of H_2O_2 (35%) to oxidize organic matter. Grain size analysis for sediments smaller than 63 μm was performed using a Mastersizer 3000 laser particle size analyzer (Malvern Panalytical B.V, Netherlands) at the Korea Polar Research Institute (KOPRI). The quality check of measurements was routinely performed by analyzing a standard sample (Quality Audit Standard for Mastersizer 3000 dispersion units, Hydro EV, QAS4002; D(10): 37.3 μm, D(50): 71.9 μm, D(90): 104.5 μm). The resulting analytical precision was as follows: D(10): 37.5 ± 0.3 μm, D(50): 71.4 ± 0.2 μm, D(90): 104.0 ± 0.0 μm.

2.4. Major element analysis

The freeze-dried subsamples (0.1 g) were completely dissolved in a 4:4:1 mixture of HNO_3, HF, and $HClO_4$. After the sample was dried on a hot-plate, refluxed several times in 6.0 M HCl to remove fluorides, and then redissolved in 5% HNO_3. The chemical composition of the inorganic phase was measured at the KBSI (Ochang Center) using inductively coupled plasma–optical emission spectroscopy (ICP–OES, OPTIMA 8300, PerkinElmer) for major elements (Al and Si). Typical uncertainties were ±5% obtained from repeated analyses of the U.S. Geological Survey basalt standard powders (BCR-2, BHVO-2, and BIR-1).

2.5. Bulk organic geochemical analysis

The freeze-dried subsamples were homogenized using an agate mortar prior to the bulk geochemical analyses. The samples were treated with 10% HCl for 24 h to remove carbonates prior to the TOC analysis. Nitrogen content was determined in a bulk sample (total nitrogen, N_{tot}) and a KOBr/KOH-treated sample (Silva and Bremner, 1966), which represented the inorganic nitrogen bound as ammonium to clay minerals (N_{inorg}). The carbon and nitrogen contents and carbon isotopic composition were determined at Hanyang University using an elemental analyzer (Euro EA3028, EuroVector, Milan, Italy) interfaced with an isotope ratio mass spectrometer (Isoprime 100, GV Instruments, UK) according to Kim et al. (2019). The carbon and nitrogen contents and their isotopic values were calibrated using two internal standards—CH6 (C = 42.1 wt%, $\delta^{13}C = -10.44$‰) and N1 (N = 21.4 wt%)—certified by the International Atomic Energy Agency (IAEA, Austria). The stable carbon isotope ratios of OC ($\delta^{13}C_{org}$) were reported using the δ notation (per mil) with respect to the Vienna Pee Dee Belemnite (VPDB). The analyses were performed at least twice, with analytical errors better than 0.05 wt% and 0.05‰ for carbon and 0.01 wt% for nitrogen. The organic nitrogen content (N_{org}) was then calculated as the difference between N_{tot} and N_{inorg} (Schubert and Calvert, 2001). Radiocarbon analyses of OC were conducted at the Alfred-Wegener-Institute (AWI, Bremerhaven, Germany) following standard procedures. Radiocarbon data were reported in the *delta* notation ($\Delta^{14}C_{org}$, ‰), as the modern fraction (Fm), and as the conventional ^{14}C age for each sample (e.g., Stuiver and Braziunas, 1993, and references therein).

2.6. Solvent-extractable lipid analysis

Lipid extraction and purification for different compound classes and analyses by gas chromatography (GC) and gas chromatography–mass spectrometry (GC–MS) were conducted at KOPRI following the procedure previously described by Kim et al. (2018; 2019). In brief, the freeze-dried and homogenized subsamples (~2 g) were extracted by sonication (dichloromethane (DCM)/methanol (MeOH); 2/1 v/v, 3 × 3 mL) and then partially purified to remove polar components and elemental sulfur using a tetrabutylammonium (TBA) sulfite reagent. Internal standards (5a-androstane and 5-α-androstan-3β-ol) were added before extraction for the quantification of *n*-alkanes and sterols, respectively. The total extracts were separated into apolar (*n*-alkanes) and polar (sterols) fractions using hexane:DCM (9/1, v/v) and DCM: MeOH (1/1, v/v), respectively. The *n*-alkanes were analyzed with an Agilent 7890B GC (Agilent Technologies, Santa Clara, CA, USA) equipped with a flame ionization detector using a DB–5 fused silica capillary column (30 m × 0.25 mm, 0.25 μm, J&W Scientific). The sterols were derivatized using N,O-bis(trimethylsilyl)trifluoroacetamide (BSTFA) and measured on an Agilent 7890B GC coupled to a 5977B Series Mass Selective Detector (Agilent Technologies, Santa Clara, CA, USA) using a DB-5 column (30 m × 0.25 mm, 0.25 μm, J&W Scientific). Errors associated with the concentrations of *n*-alkanes and sterols were typically <10% based on the replicate analysis of the same sediment sample.

2.7. CuO oxidation product analysis

CuO oxidation of sediment samples and analyses by GC–MS were conducted at the Institute of Marine Sciences-National Research Council (ISMAR-CNR) according to the method described by Tesi et al. (2014). Briefly, the freeze-dried and homogenized subsamples (~300 mg) were mixed with 300 mg of cupric oxide (CuO), 50 mg of ammonium iron (II) sulfate hexahydrate ($Fe(NH_4)_2(SO_4)_2{\cdot}6H_2O$), and 20 mL of 2 M N_2-purged NaOH solution in Teflon tubes. Microwave-assisted alkaline CuO oxidation was carried out using a MARS6 microwave at 150 °C for 1.5 h. After oxidation, a known amount of an internal recovery standard (ethyl vanillin and cinnamic acid) was added. Afterward, the samples were acidified with concentrated HCl to pH 1, and phenols were extracted twice from the water phase using ethyl acetate (EtOAc). After removing residual water from the supernatant using anhydrous sodium sulfate (Na_2SO_4), the solvent was evaporated under N_2, and the samples were redissolved in pyridine. Prior to the analyses, the oxidation products were derivatized with BSTFA and 1% trimethylchlorosilane (TMCS) at 60 °C for 1 h to yield trimethylsilyl derivatives. The molecular composition was examined on an Agilent 7820A GC coupled to a 5977B Series Mass Selective Detector (Agilent Technologies, Santa Clara, CA, USA) in single ion monitoring (SIM) mode using a DB1-MS capillary column (30 m × 0.25 mm, 0.25 μm, Agilent J&W). Errors associated with phenol concentration data were typically <10% based on the replicate analysis of the same sediment sample.

3. Results

3.1. Sediment properties

The mineral-specific SA values ranged from 28 to 41 m^2/g (mean ± standard deviation; 37 ± 4 m^2/g), showing an increasing trend with water depth (Table S1). The surface sediments were predominantly composed of silt (48 ± 8%) and clay (51 ± 9%), with a minor sand proportion of 0.1–2.8% (0.8 ± 1.1%) (Table S1). Generally, the silt percentage decreased and the clay percentage increased with water depth. The mean grain size varied between 2.4 and 6.5 μm (3.6 ± 1.5 μm) and decreased with water depth. The Al and Si concentrations varied between 6.6% and 7.6% (7.1 ± 0.4%) and between 23.6% and 27.0% (25.2 ± 1.1%), respectively (Table S1), and the Al/Si ratio showed an increasing trend with water depth.

3.2. Elemental and isotopic compositions

The TOC contents were similar along the Mackenzie Trough, ranging from 1.6 to 2.0 wt% (1.8 ± 0.1 wt %) (Fig. 2A). The total nitrogen (N_{tot}) content varied between 0.15 wt% and 0.20 wt% (0.18 ± 0.02 wt %), while the total organic nitrogen (N_{org}) contents were one order lower (0.06 ± 0.02 wt %) and showed an increasing trend with water depth (Fig. 2B). Thus, the organic fraction accounted for only 22–41% of the N_{tot}. The TOC/N_{tot} ratios (commonly quoted as C/N) were between 8.7 and 11.3 (9.9 ± 0.8), while the TOC/N_{org} ratios were much higher at values of 22.9–52.3 (32.4 ± 10.8). Similarly, the molar N_{tot}/TOC ratios (0.12 ± 0.01) were different from the molar N_{org}/TOC ratios (0.03 ± 0.01) and showed an increasing trend with distance offshore (Fig. 2C). The $\delta^{13}C_{org}$ values varied between −26.7‰ and −24.7‰ (−25.7 ± 0.6‰), showing a clear increasing trend with water depth (Fig. 2D). Similarly, the $\Delta^{14}C_{org}$ values increased from −733.7‰ to −586.2‰ (−627.5 ± 48.1‰) with water depth (Fig. 2D).

3.3. Solvent-extractable lipid signatures

Solvent-extractable *n*-alkanes were detected in a series of C_{15} to C_{35}, with a predominance of *n*-C_{27}, *n*-C_{29}, and *n*-C_{31} homologues. The concentrations of odd-carbon-numbered HMW *n*-alkanes in C_{25}–C_{33} normalized to SA ranged from 0.14 to 1.44 μg/m^2 (0.44 ± 0.44 μg/m^2) and decreased with distance offshore (Fig. 3A). In contrast, the odd-carbon-numbered low molecular weight (LMW) *n*-alkanes in $C_{17–19}$ normalized to SA showed no clear trends, with values of 0.01–0.03 μg/m^2 (0.02 ± 0.01 μg/m^2). The average chain length (ACL) of HMW *n*-alkanes ($ACL_{25–33}$), calculated according to Cranwell et al. (1987), was relatively stable along the transect, with an average length of 29.4 ± 0.3. The carbon preference index (CPI) of HMW *n*-alkanes ($CPI_{25–33}$), calculated according to Bray and Evans (1961), ranged from 1.7 to 3.1 (2.2 ± 0.5). The SA-normalized concentrations of brassicasterol and cholesterol were between 1.4 and 16.9 μg/m^2 (6.1 ± 6.2 μg/m^2) and between 2.5 and 54.2 μg/m^2 (16.6 ± 19.0 μg/m^2), respectively, with higher values at the offshore sites (Fig. 3B).

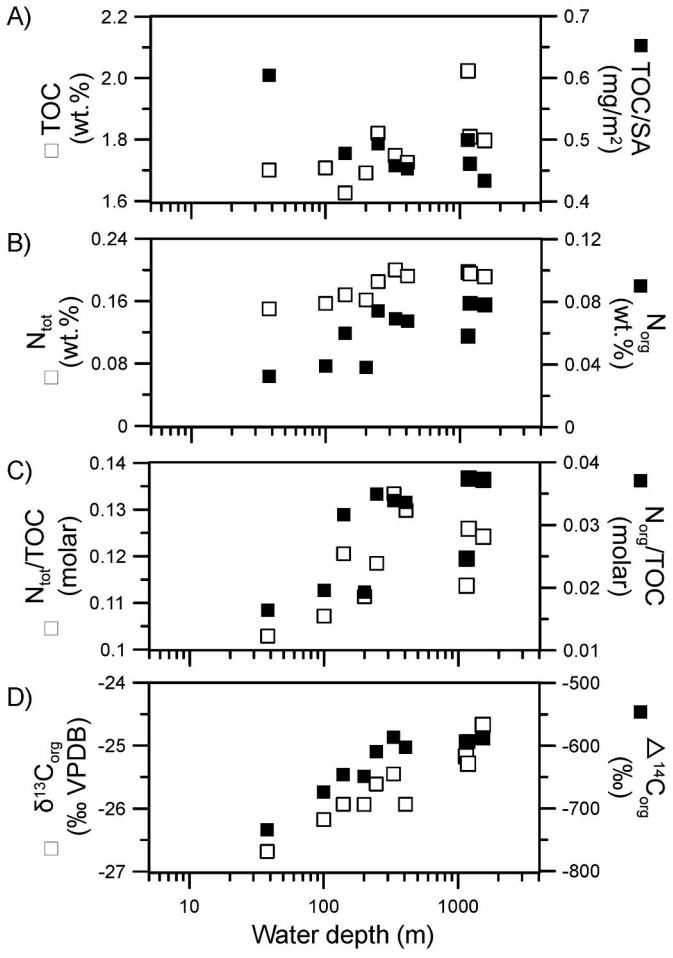

Fig. 2. Variations in A) TOC content (wt.%) and TOC/SA ratio (mg/m^2), B) N_{tot} and N_{org} content (wt.%), C) molar N_{tot}/TOC and N_{org}/TOC ratios, and D) $\delta^{13}C_{org}$ (‰ VPDB) and $\Delta^{14}C_{org}$ (‰) with water depth.

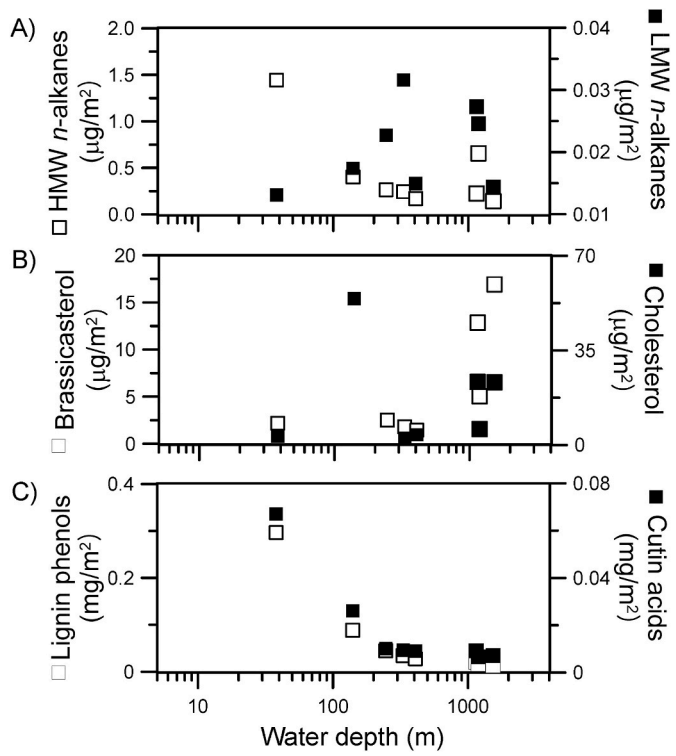

Fig. 3. Variations in biomarker concentrations normalized by SA: A) HMW and LMW *n*-alkanes (μg/m^2), B) brassicasterol and cholesterol (μg/m^2), and C) lignin phenols and cutin acids (μg/m^2) with water depth.

3.4. CuO oxidation product signatures

The results of lignin phenols and cutin acids obtained from the alkaline CuO oxidation of surface sediments are presented in Fig. 3C (see also Table S2). We reported total lignin phenol concentrations as the sum of eight lignin-derived monomeric phenols, including vanillyl (V; vanillin, acetovanillone, and vanillic acid), syringyl (S; syringaldehyde, acetosyringone, and syringic acid), and cinnamyl (C; p-coumaric acid and ferulic acid) units normalized to SA. Total cutin acid concentrations were also reported as the sum of seven aliphatic lipids, including ω-hydroxyhexadecanoic acid, 8,9,10,ω-hydroxyhexadecanoic acid, x-Hydroxyhexadecan-1,16-dioic acid, and 7,8x-Hydroxyhexadecan-1,16-dioic acid. The concentrations of lignin phenols and cutin acids were 0.01–0.30 mg/m^2 (0.07 ± 0.10 mg/m^2) and 0.01–0.07 mg/m^2 (0.02 ± 0.05 mg/m^2), respectively, and showed decreasing trends with water depth (Fig. 3C, see also Table S2). The syringyl-to-vanillyl phenol (S/V) and cinnamyl-to-vanillyl phenol (C/V) ratios were 0.5–0.7 (0.6 ± 0.1) and 0.2–0.8 (0.4 ± 0.2), respectively (Table S2). The acid-to-aldehyde (Ad/Al) ratios of vanillyl (V) phenols ((Ad/Al)v) varied between 0.41 and 0.76 (0.62 ± 0.11) (Table S2). CuO oxidation also releases 3,5-dihydroxybenzoic acid (3,5-Bd), and the ratio of the 3,5-Bd to vanillyl phenols (3.5-Bd/V) varied between 0.11 and 0.28 (0.19 ± 0.06) (Table S2).

4. Discussion

4.1. Controls on organic carbon loading

The TOC values obtained from the Mackenzie Trough transect were in the range of 1.6–2.0 wt% (1.7 ± 0.1 wt%) (see Table S1), which were similar to those previously reported for the Mackenzie Shelf and the Beaufort slope (0.9–2.0 wt%, 1.4 ± 0.2 wt%) Drenzek et al. (2007); Magen et al. (2010); Goñi et al. (2013); Vonk et al. (2015). The TOC content showed no clear trend with water depth (Fig. 2A), while SA showed a generally increasing trend with water depth; this resulted in a decrease in the TOC/SA ratio ($R^2 = 0.58$, $p < 0.001$) (Fig. 2A), which is typically referred to as "OC loading" (Keil et al., 1997). We observed a general decrease in sediment mean grain size with water depth, which showed a broad negative relationship with SA ($R^2 = 0.94$, $p < 0.001$) (Fig. 4A). Hydrodynamic sorting during sediment transport likely affected the particle size distribution, resulting in the accumulation of fine-grained sediments with higher SA at deeper water depths. We also identified positive relationships between SA and clay percentage ($R^2 = 0.91$, $p < 0.001$) (Fig. 4B) and between SA and Al/Si ($R^2 = 0.69$, $p < 0.001$) (Fig. 4C). Hence, the shallower samples with lower SA were relatively quartz-rich (lower Al/Si), whereas the deeper samples were clay-rich (higher Al/Si). Our results are consistent with a previous study that showed a general increase in the Al/Si ratio and thus a general decrease in sediment grain size from the Mackenzie River channels to the Mackenzie Shelf (Vonk et al., 2015). Accordingly, the increase in SA and clay with water depth indicates the preferential transport of fine-grained clay-rich particles which caused the decrease in TOC/SA and thus OC loading with distance offshore. Hence, our results highlight the important role of hydrodynamic sorting on OC loading along the Mackenzie Trough transect.

The Mackenzie Trough and shelf sediment TOC/SA ratios (Fig. 4D) were generally within the range of 0.4–1.0 mg/m^2 (e.g., Keil et al., 1994; Mayer, 1994; Blair and Aller, 2012), which suggests that the supply and decomposition of OC were relatively balanced. However, the TOC contents of sediments at deeper water depths in the Mackenzie Trough transect were weakly controlled by SA (Fig. 4D). Our results are in line with those of previous studies on the Beaufort slope (Goñi et al., 2013; Vonk et al., 2015). This observation suggests that another factor, in addition to hydrodynamic sorting, may have controlled OC loading. TOC/SA ratios of less than 0.4 mg/m^2 generally correspond to deeper ocean sediments with long oxygen exposure times (e.g., Aller and Blair, 2006). For example, a previous study (Goñi et al., 2013) identified OC loadings of <0.4 mg/m^2 with > 5-cm-thick Mn layers in deep water (>500 m) samples from the Beaufort slope, which suggests deeper oxygen penetration and thus longer oxygen exposure times. Exposure to efficient oxidants exerts first-order control on OC degradation by metabolic processes during cross-shelf transport and seafloor deposition (e.g., Hartnett et al., 1998; Hedges et al., 1999; Keil et al., 2004; Meile and van Cappellen, 2005). Hence, the general decrease in TOC/SA along the Mackenzie Trough transect may be partly due to OC degradation during transport and/or within the seabed.

4.2. Source and degradation status of sedimentary organic carbon on a bulk level

Previous work conducted along the North American Arctic margin showed a significant linear correlation between TOC and N_{tot}, with a very small N_{tot} intercept at 0 wt% of TOC (Goñi et al., 2013). However, the N_{tot} versus TOC plot in this study inferred substantial proportions of sediment-bound inorganic N in the Mackenzie Trough transect (Fig. 5A), accounting for up to 80% of N_{tot}, which is comparable to previously reported values (28–63%) in the central Arctic Ocean (Schubert and Calvert, 2001). The presence of bound inorganic N may be explained by the high clay content in sediments (average of 51 ± 9%, see Table S1). The N_{tot}/TOC molar ratios (Fig. 5B), commonly used for discriminating marine from terrestrial organic matter in sediments, were much higher than the N_{org}/TOC molar ratios (data not shown). Notably, the N_{tot}/TOC values obtained in this study (0.118 ± 0.010) were similar to those obtained in previous studies (0.111 ± 0.038) in the Beaufort Sea (see Fig. 5B). It is therefore necessary to consider the presence of inorganic nitrogen bound in clay minerals to better characterize sedimentary OC sources (using N_{org} rather than N_{tot} to calculate N/C ratios) (Schubert and Calvert, 2001; Knies et al., 2007).

The surface sediments from the Mackenzie Trough transect displayed relatively depleted $\delta^{13}C_{org}$ values (<−24‰, see Fig. 2D). Notably, the $\delta^{13}C_{org}$ compositions determined in this study were comparable to those in surface sediments from the Beaufort Sea (Fig. 5C). These $\delta^{13}C_{org}$ compositions are typical of C_3 terrestrial plants (e.g., Goñi et al., 2005). Surface sediment OC from the Mackenzie Trough transect was also characterized by depleted ^{14}C values (−586‰ to −734‰, see Fig. 2D). The ranges in $\Delta^{14}C_{org}$ compositions observed in our study were also within the range of those reported previously in the Beaufort Sea (Fig. 5C). In general, the $\delta^{13}C$ values of Mackenzie Delta particulate organic carbon (POC) were more depleted (−26.2‰ to −26.9‰, Goñi et al., 2005; Hilton et al., 2015) than those of marine OC (15.6‰ to

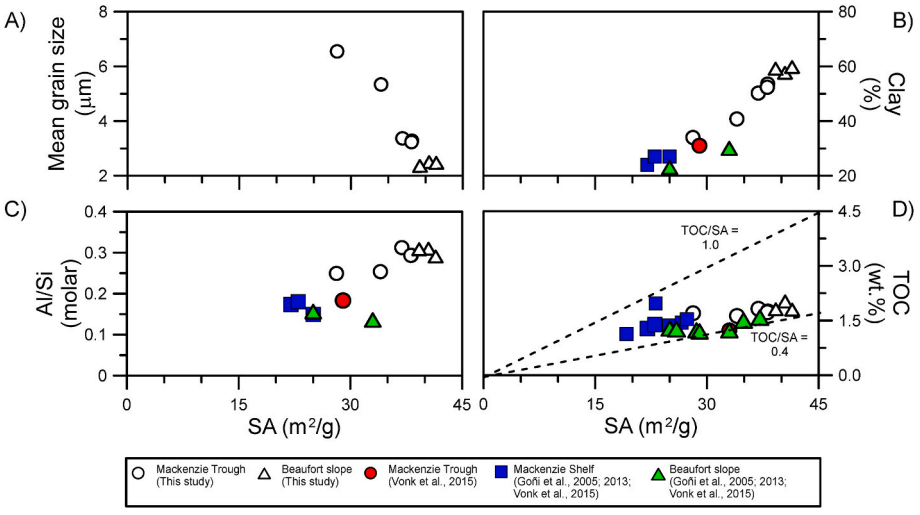

Fig. 4. Scatter plots of SA (m^2/g) with A) mean grain size (μm), B) clay percentage (%), C) molar Al/Si ratio, and D) TOC (wt.%). The range (0.4–1.0 mg/m^2) of OC loading (TOC/SA) trends commonly observed in river sediments (Blair and Aller, 2012) is also shown.

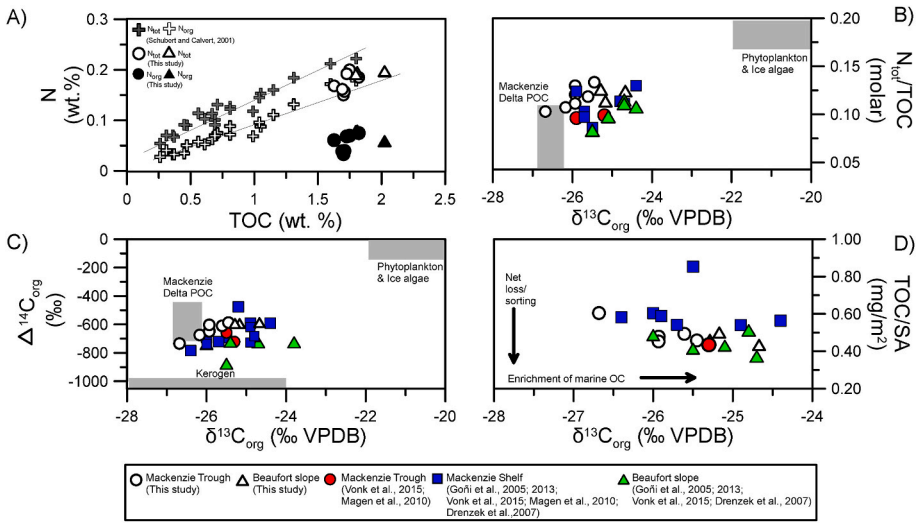

Fig. 5. Scatter plots of A) TOC (wt.%) vs. N_{tot} or N_{org} (wt.%), and $\delta^{13}C_{org}$ (‰ VPDB) with B) molar N_{tot}/TOC, C) $\Delta^{14}C_{org}$ (‰), and D) TOC/SA (mg/m^2). The compositional ranges of particulate organic carbon (POC) from the Mackenzie Delta (Goñi et al., 2005; Hilton et al., 2015), bedrock-derived kerogen, and marine phytoplankton and ice algae (Schubert and Calvert, 2001) are also shown in the plots. Note that the $\Delta^{14}C_{org}$ compositional ranges of phytoplankton and ice algae are assumed to reflect the ^{14}C compositions of dissolved inorganic carbon in regional surface waters (e.g., Griffith et al., 2012).

−18.3‰, Schubert and Calvert, 2001). The reported $\Delta^{14}C_{org}$ values were from −436‰ to −714‰ for the Mackenzie Delta POC (Goñi et al., 2005; Hilton et al., 2015) and from 19‰ to −112‰ for marine phytoplankton and ice algae; the $\Delta^{14}C_{org}$ ranges of marine phytoplankton and ice algae are assumed to reflect the ^{14}C compositions of dissolved inorganic carbon in regional surface water (Griffith et al., 2012; Goñi et al., 2013; Druffel et al., 2017). The $\delta^{13}C_{org}$ and $\Delta^{14}C_{org}$ data therefore suggest that surface sediments from the Mackenzie Trough transect were enriched in terrestrial OC (Fig. 5C). A scatter plot of $\delta^{13}C_{org}$ versus TOC/SA (Fig. 5D) was used to distinguish two processes: (1) a net loss of terrestrial OC caused by either hydrodynamic sorting or degradation and (2) replacement of terrestrial OC with autochthonous marine OC during OC transport (Bröder et al., 2016). As also indicated by the SA versus TOC scatter plot (see Fig. 5D), the TOC/SA appears to decrease along the Mackenzie Trough transect, partly due to OC degradation. However, the increasing $\delta^{13}C_{org}$ values indicate the enrichment of sedimentary OC with autochthonous marine OC as a function of water depth. Notably, the bulk OC age decreased with increasing water depth from ~10563 to ~7048 ^{14}C years (see Table S1), which further supports increasing proportion of autochthonous marine OC with younger ^{14}C ages in sedimentary OC.

4.3. Source and degradation status of sedimentary organic carbon on a molecular level

The odd-carbon-numbered HMW *n*-alkanes (>C_{25}) are typical of terrestrial vascular plant inputs (e.g., Eglinton and Hamilton, 1967). The concentrations of HMW *n*-alkanes decreased with water depth along the Mackenzie Trough transect (Fig. 3A). Lignin-derived vanillyl, syringyl, and cinnamyl phenols are characteristic of different terrestrial vascular plant sources (e.g., Hedges and Mann, 1979), whereas cutin-derived hydroxy fatty acids are characteristic of soft aerial (leaves and needles) and subaerial (root) tissues in vascular plants (e.g., Goñi and Hedges, 1990). We observed exponential decreases in lignin phenols and cutin acids with water depth (Fig. 3C), similar to that of HMW *n*-alkanes (Fig. 3A). These trends were consistent with terrestrial biomarker data normalized by sediment dry weight (see Fig. S1) and TOC (see Fig. S2). The lignin source indicators S/V and C/V were used to determine the relative input of non-woody angiosperm to the woody gymnosperm input (Hedges and Mann, 1979; Goñi and Hedges, 1995). The lignins in the Beaufort Sea (Fig. 6A) were found to be a mixture of gymnosperm wood-derived OC with inputs from angiosperm non-woody tissues (Hedges and Mann, 1979; Goñi and Hedges, 1995; Keil et al., 1998). The OC-normalized yields of lignin phenols from the Mackenzie Trough transect (0.2–4.4 mg/gTOC, see Table S2) were within the reported

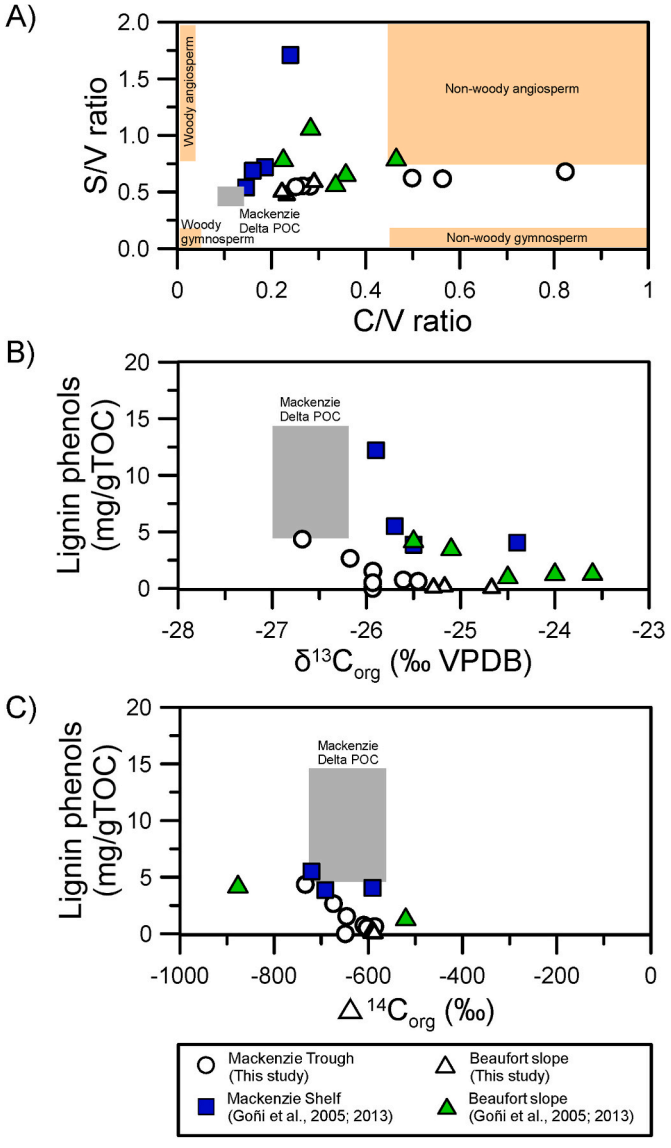

Fig. 6. Scatter plots of A) S/V vs. C/V with the endmembers for different vascular plant tissues (cf. Goñi et al., 2000), B) $\delta^{13}C_{org}$ (‰ VPDB) vs. lignin phenols (mg/gTOC), and C) $\Delta^{14}C_{org}$ (‰) vs. lignin phenols (mg/gTOC).

range of suspended particulate matter (SPM) from the Mackenzie Delta (5.4–14.3 mg/gTOC; Goñi et al., 2000, 2005) and of surface sediments from the Mackenzie Shelf and Beaufort slope (1.2–12.2 mg/gTOC; Goñi et al., 2005, 2013). Overall, lignin phenols showed negative relationships with $\delta^{13}C_{org}$ and $\Delta^{14}C_{org}$ (Fig. 6B and C). These patterns provide additional evidence for the decreased contribution of terrestrial OC to sedimentary OC due to the replacement of younger marine OC.

The odd-carbon-numbered LMW *n*-alkanes (C_{15} to C_{19}) are mostly from aquatic algal and photosynthetic bacterial inputs (e.g., Han and Calvin, 1969; Meyers and Ishlwatari, 1993). The concentrations of LMW *n*-alkanes were variable (Fig. 3A), which resulted in the increase of LMW to HMW *n*-alkanes with water depth (see Table S2). This suggests a decreasing proportion of terrestrial OC to sedimentary OC with increasing water depth due to the input of marine OC. Brassicasterol and cholesterol are dominant in invertebrates and marine zooplankton (Derrien et al., 2015) and are therefore indicative of marine-derived OC. In particular, brassicasterol can be used as a phytoplankton biomarker for marine diatoms, although it can also be derived from terrestrial sources (e.g., Huang and Meinschein, 1976; Volkman, 1986; Ding et al., 2017). Therefore, the generally higher concentrations of both brassicasterol and cholesterol at the deeper water sites (see Fig. 3B) are in line with the decreasing HMW *n*-alkane and lignin phenols concentrations with water depth. This suggests that the contribution of marine OC to sedimentary OC increased with distance offshore due to the enrichment of marine OC.

The *n*-alkane distributions may change over the course of post-depositional degradation (e.g., Buggle et al., 2010) and can therefore be used as an indicator of hydrocarbon biodegradation and maturity (e.g., Cranwell, 1981; Huang et al., 1996). The $CPI_{25–33}$ of HMW *n*-alkanes decreased with water depth (Fig. 7A), indicating increasing hydrocarbon alteration with increasing water depth. The (Ad/Al)v ratio can be used as an indicator of lignin degradation because acidic phenols are produced from aldehyde functional groups through propyl side-chain oxidation (e.g., by white-rot decay) during lignin degradation (e.g., Hedges and Ertel, 1982; Ertel et al., 1986; Goñi and Hedges, 1992; Opsahl and Benner, 1995; Otto and Simpson, 2006). The (Ad/Al)v ratios were higher at deeper water depths (Fig. 7B, see also Fig. S3), indicating enhanced side-chain oxidation of lignins with increasing water depth. In comparison, 3,5-Bd is a common product of soil degradation processes and is thus most enriched in soils (e.g., Prahl et al., 1994; Goñi et al., 2000; Houel et al., 2006; Otto and Simpson, 2006). The 3,5-Bd/V ratio has therefore been used to characterize the degradation state of complex terrestrial organic mixtures (e.g., Prahl et al., 1994) and trace inputs of soil OC to sediments (e.g., Louchouarn et al., 1999; Dickens et al., 2007). The ratio of 3,5-Bd/V also increased with water depth in this study (Fig. 7C, see also Fig. S3), indicating an increase in the contribution of degraded OC to sedimentary OC with distance offshore; this is likely linked to an increase in the proportion of soil-derived OC to terrestrial OC relative to that of fresher vascular plant tissues. Furthermore, the ratio of HMW *n*-alkanes/lignin phenols increased with increasing water depth (Fig. 7D) and decreasing grain size (see Table S1). Our results therefore indicate the preferential offshore transport of more degraded terrestrial OC (e.g., HMW *n*-alkanes) selectively bound to fine-grained sediments, while less degraded terrestrial OC (e.g., lignins) was retained near the coast.

4.4. Burial efficiency of terrestrial organic carbon

A gradual increase in $\delta^{13}C_{org}$ with water depth (see Fig. 2D) coincided with the decrease in TOC/SA ratios (see Fig. 2A), indicating the simultaneous loss of terrestrial OC and replacement with marine OC with increasing water depth. The decrease in TOC/SA along the Mackenzie Trough transect can be used to calculate the burial efficiency (BE; defined as the ratio of the amount of terrestrial OC that is buried in marine sediments to what arrives at the delta head) of terrestrial OC, similar to the work by Vonk et al. (2015). The fraction of terrestrial OC (F-terr) to TOC was determined by source apportionment calculations using the $\delta^{13}C$ data as follows:

$$\delta^{13}C_{org}\ \text{of sediment} = \text{F-marine} \times \delta^{13}C_{marine} + \text{F-terr} \times \delta^{13}C_{river}. \quad (1)$$

Here, we used a $\delta^{13}C_{river}$ value of −26.5 ± 0.2 (Mackenzie Delta suspended sediments, n = 12; Goñi et al., 2005; Hilton et al., 2015) and a $\delta^{13}C_{marine}$ of −20.2 ± 1.7‰ (Goñi et al., 2000). The F-terr decreased from 103% to 71% with increasing water depth (see Table S3). The fraction of the remaining surface loading (F-rsl) was derived from the decrease in SA, as follows:

$$\text{F} - \text{rsl} = \frac{\text{TOC/SA of sediment}}{\text{TOC/SA of river suspended sediment}} \quad (2)$$

here, we used the published TOC/SA value of 0.78 ± 0.06 mg/m^2 (n = 4) obtained from suspended sediment samples collected from Mackenzie Delta channels (Goñi et al., 2005). The F-rsl also decreased from 78 ± 6% to 56 ± 6% with increasing water depth (see Table S3). The BE of riverine OC in delta systems is a product of the fraction of the remaining surface loading (F-rsl) and the fraction of terrestrial OC in TOC (F-terr) (Keil et al., 1997). Thus, the BE of terrestrial OC was then determined by multiplying the F-terr with F-rsl as follows:

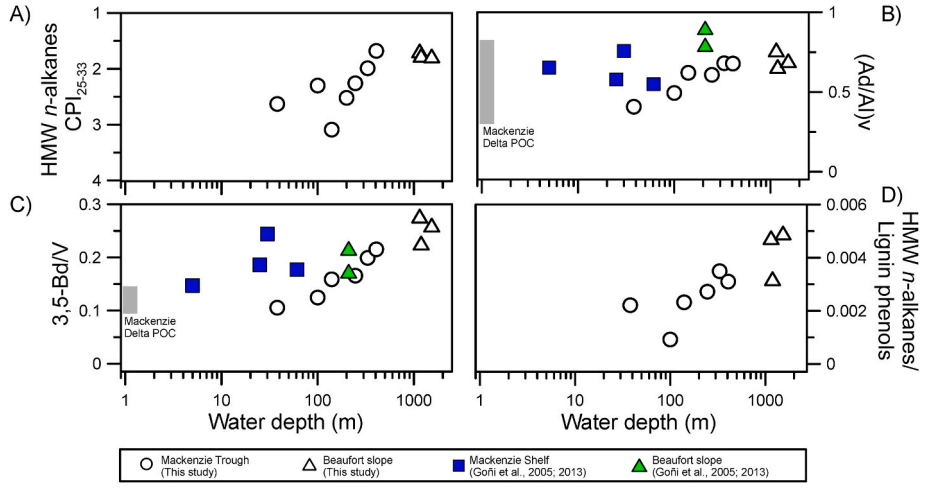

Fig. 7. Variation in degradation indices of terrestrial biomarkers: A) carbon preference indices of HMW *n*-alkanes (CPI_{25-33}), B) (Ad/Al)v, C) 3,5-Bd/V, and D) HMW *n*-alkanes/lignin phenols.

BE = F-terr x F-rsl. (3)

The BE varied between 39 ± 6% and 80 ± 6% (see Table S3), with lower values for samples farther from the trough head (see Fig. S4). Overall, these estimates suggest that approximately 61 ± 6% of terrestrial OC in the Mackenzie River was lost during transport along the Mackenzie Trough. We compared our results with those previously reported for the Mackenzie Shelf and Beaufort slopes (Goñi et al., 2005, 2013; Vonk et al., 2015). The BE for the Mackenzie Shelf was between 52 ± 15% and 73 ± 15%, and that for the Beaufort slope was between 34 ± 6% and 48 ± 6% (Fig. 8A, see also Table S3). We observed a similar range of BEs between the Mackenzie Trough and Shelf samples but lower BEs for the Beaufort slope. Interestingly, the BE of sediments at site SS4 (45 ± 3%) collected in 1987 using a Smith–McIntyre grab sampler (Yunker et al., 1990) was slightly lower than that at site ARA05C-34BC (54 ± 4%) collected in 2014 (see Fig. 1). However, our data comparison is limited due to the low coverage of sediment organic data in the Mackenzie Trough. Nonetheless, our study suggests that the BE of terrestrial OC is slightly greater in the Mackenzie Trough than in the surrounding continental slope.

4.5. Contribution of biogenic versus petrogenic OC

Modern sediment supply to the Mackenzie Shelf is dominated by the Mackenzie River (Hill et al., 1991). The input of ice-bearing unconsolidated sediments from coastal bluff erosion to the Beaufort Sea is only ~1% of the sedimentary input of the Mackenzie River (i.e. 1.25 Tg/yr; Hill et al., 1991). Thus, the Mackenzie River is the primary terrestrial OC source to the Mackenzie Trough (e.g., Macdonald et al., 1998; McMahon et al., 2021). The $\Delta^{14}C_{org}$ values increased along the Mackenzie Trough with water depth with the most negative $\Delta^{14}C_{org}$ value (−734‰) at the head of the Mackenzie Trough, i.e., close to the delta (see Fig. 2D). Notably, this value was substantially older (10563 ^{14}C yr BP) than those reported for suspended sediments in the Mackenzie Delta (−622 ± 36‰), with an average age of 7892 ± 1464 ^{14}C yr BP (n = 11; Goñi et al., 2005; Hilton et al., 2015). The older OC in the Mackenzie Trough in comparison to the deltaic suspended sediments could be due to the ageing of OC during its transport, possibly due to the preferential degradation of labile OC with younger ^{14}C signal. Previous studies inferred the transport of petrogenic OC (sometimes termed "ancient" OC, "fossil" OC, or "rock-derived" OC) to the Beaufort Sea via the Mackenzie River, mainly as eroded Devonian shales, coals, or immature bitumens. This recalcitrant material is also preferentially preserved over more labile, plant-related terrestrial debris (Yunker et al., 2002, 2011; Goñi et al., 2005; Drenzek et al., 2007). Thus, our results highlight the need to further characterize OC to better constrain the fresher, more labile biogenic fraction of sedimentary OC in the Canadian Beaufort Sea.

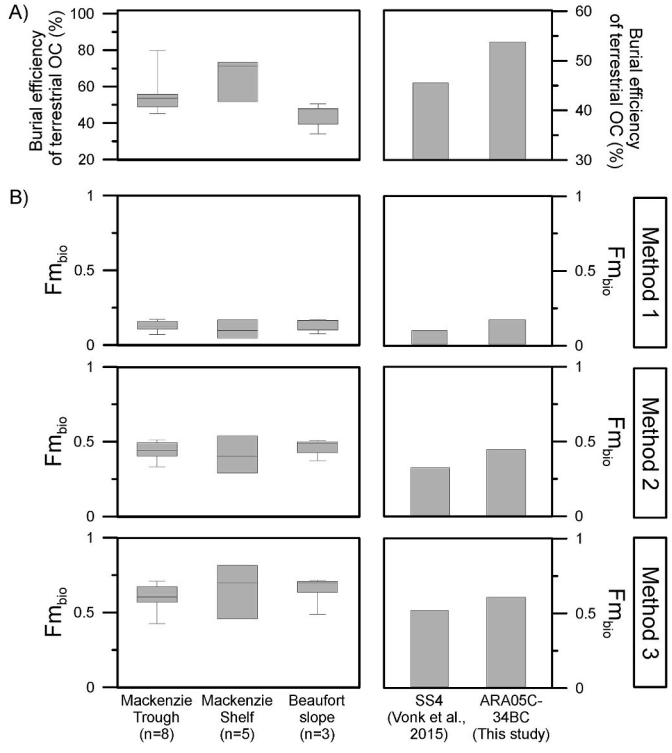

Fig. 8. Estimates of A) the burial efficiency of terrestrial OC and B) the ^{14}C composition of the biogenic OC fraction (Fm_{bio}) derived from three different methods in the Mackenzie Trough, Mackenzie Shelf, and Beaufort slope. The burial efficiency and Fm_{bio} were also compared for sites SS4 and ARA05C-34BC collected in 1987 and 2014, respectively.

For this purpose, we applied three different methods to calculate the relative proportions of "^{14}C-assessed" biogenic and petrogenic OC. First, we estimated the amount of "petrogenic" OC added to sedimentary OC using a simple binary mixing model (Method 1), as the more recently fixed "biogenic" (modern terrestrial, riverine, and marine) OC has a young ^{14}C age. We assumed the end-member $\Delta^{14}C$ values to be $\Delta^{14}C_{petrogenic} = -1000‰$ and $\Delta^{14}C_{biogenic} = 0‰$ (cf. Goñi et al., 2005). The biogenic OC fraction of TOC (F-bio in %) was 27–41% along the Mackenzie Trough transect (see Table S3), which was comparable to the published data from the Beaufort Sea using the same approach (Goñi et al., 2005; Vonk et al., 2015). Subsequently, the ^{14}C composition of F-bio (referred as Fm_{bio}) was 0.07–0.17 in the Mackenzie Trough, 0.05–0.17 in the Mackenzie Shelf, and 0.07–0.17 in the Beaufort slope (Fig. 8B). However, defining biogenic OC with a $\Delta^{14}C$ of 0‰ is likely too simplistic, as biogenic OC consists of a large mixture of pre-aged OC with above-ground biomass (C_3 and C_4-plants) and riverine/marine autotrophic organisms (e.g., Hilton et al., 2010).

Second, we defined the two unknown components as "petrogenic" OC and "biogenic" OC derived from modern biomass (i.e., more recently fixed terrestrial, riverine, and marine biomass) and pre-aged soils. We then calculated the relative OC proportions to sedimentary OC by applying a binary mixing model (Method 2) as follows (cf. Galy et al., 2008):

$$TOC_{sample} \times Fm_{sample} = TOC_{sample} \times Fm_{bio} - OC_{petro} \times Fm_{bio} \quad (4)$$

where TOC_{sample} is the TOC content in the sample as a percentage of the dry weight (that is, wt.%), Fm_{sample} is the measured ^{14}C composition of the sample expressed as the fraction of modern C, Fm_{bio} is the ^{14}C composition of biogenic OC, and OC_{petro} is the content of petrogenic OC in wt.%. The relationship between $TOC_{sample} \times Fm_{sample}$ (y-axis) and TOC_{sample} (x-axis) was strongly linear ($y = 0.6338 \times x - 0.4347$, $R^2 = 0.71$, $p < 0.001$, n = 40; Fig. 9A), which suggests that the proportion of petrogenic OC was relatively invariant. The OC_{petro} value, which was determined as the intercept between the regression line and the x-axis (i.e., the value for $y = 0$), was 0.43 wt%. Fm_{bio} was 0.43 ± 0.06 in the Mackenzie Trough transect, with corresponding F-bio values of 41–59% (see Table S3). As illustrated in Fig. 8B, the resultant Fm_{bio} values were higher than those calculated via Method 1, as the biogenic OC is much older than the previous assumption (i.e., $\Delta^{14}C = 0‰$).

For the third approach (Method 3), we used Al/TOC ratios and Fm_{sample} values to determine the fraction of modern and pre-aged "biogenic" and "petrogenic" OC (cf. Dellinger et al., 2014; Hilton et al., 2015; Vonk et al., 2015). Using data from this study and from Vonk et al. (2015), the Al/TOC ratio of petrogenic bedrock was obtained as the intercept at Fm = 0 (Fig. 9B). We then used the Al content (ppm) of the samples (74322 ± 14606 ppm, n = 24; Dellinger et al., 2014) to calculate an OC_{petro} of 0.42 wt%. We calculated the petrogenic OC fraction of TOC (F-petro in %) using TOC_{sample} (wt.%) and OC_{petro} (wt.%) values. The Fm_{bio} was obtained as follows:

$$Fm_{sample} = F-bio(\%) \times Fm_{bio} + F-petro(\%) \times Fm_{petro} \quad (5)$$

where F-bio (%) = (100 – F-petro (%)), as F-petro is known and Fm_{petro}

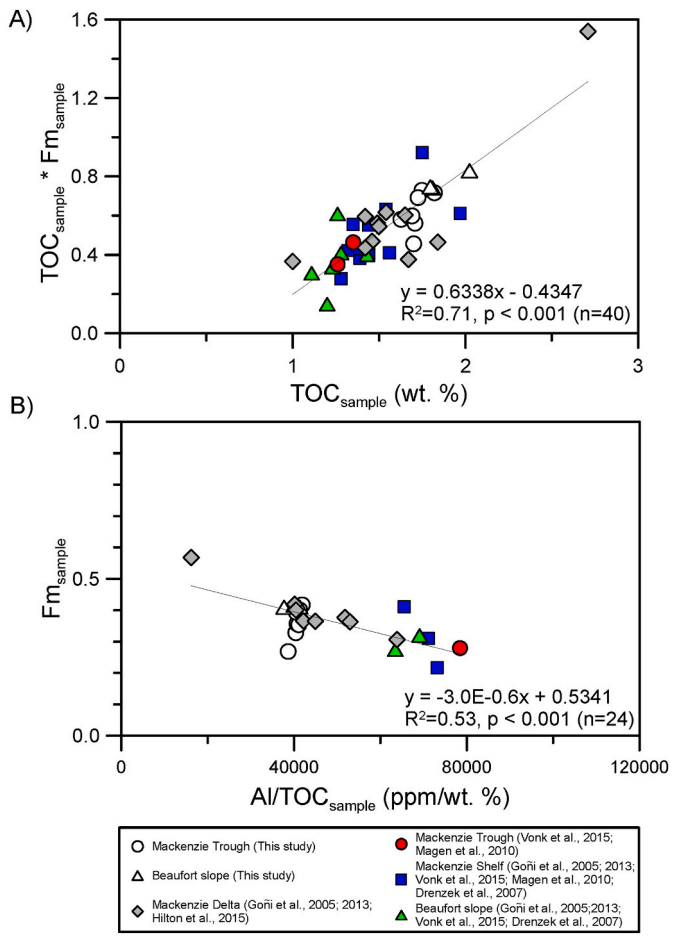

Fig. 9. Scatter plots of A) TOC_{sample} (wt. %) vs. TOC_{sample}*Fm_{sample}, and B) Al/TOC (ppm/wt. %) vs. Fm.

= 0. The F-bio in the Mackenzie Trough transect was between 45% and 63% (see Table S3). The resultant Fm_{bio} values were 0.60 ± 0.09 in the Mackenzie Trough transect, showing a decreasing trend with water depth (see Fig. S4B). Similar to the results from Methods 1 and 2 (see Fig. 8B), the median value of Fm_{bio} was lower in the Mackenzie Trough than in the Beaufort slope, suggesting the higher contribution of marine OC to sedimentary OC in the Beaufort slope.

Interestingly, all three methods showed lower biogenic OC contributions in samples collected from site SS4 in 1987 (using a Smith–McIntyre grab sampler; Yunker et al., 1990) than that at site ARA05C-34BC collected in 2014 (using a box corer; see Table S3); however, small differences were observed between the methods. Consequently, the Fm_{bio} values were higher at site ARA05C-34BC than at site SS4 (see Fig. 8B). Thus, our results hint that the biogenic OC contribution to sedimentary OC might have increased in the Mackenzie Trough in recent years. Given that the ^{14}C-depletion of OC in the Mackenzie River is mainly attributed to the erosion of pre-aged permafrost soils (Hilton et al., 2015), we speculated that the land–ocean OC transfer increased due to strengthened permafrost thawing in response to recent Arctic warming, which further enhanced the BE of terrestrial OC. The increased burial of terrestrial OC would have shortened the exposure time of sedimentary OC to oxygen, which hampered terrestrial OC degradation and thus resulted in younger ^{14}C ages of sedimentary OC. The lower mean monthly water discharge from the Mackenzie River (at the GRDC station) in 1987 (8657 m^3/s) compared with that in 2014 (9831 m^3/s) (http://www.bafg.de/GRDC/EN/01+GRDC/13_dtbse/database_node.html) further supports the enhanced land–ocean OC transfer. It is worth noting that nutrient inputs from the Mackenzie River elicits large primary production and high sinking particulate fluxes near the Mackenzie River delta especially in late spring and summer (e.g., Stein and MacDonald, 2004; O'brien et al., 2006; McMahon et al., 2021). Hence, alternatively, the increased supply of nutrient-rich freshwater from the Mackenzie River could have enhanced primary production in the Beaufort Sea, which might have attributed to the relatively young ^{14}C ages of sedimentary OC. However, considering that the burial efficiency of terrestrial OC was higher in the sample collected in 2014 than in 1987 (Fig. 8A), the younger age of OC for the sample collected in 2014 was more probably due to the increase of terrestrial OC rather than marine OC. Consequently, the increasing transfer of permafrost-derived biogenic OC to the Canadian Beaufort Sea should be considered in future regional carbon budget calculations. Nonetheless, we should also note that the grab sampler does not preserve the sediment-water interface. Thus, the sample SS4 could include deeper sediment layers that contain lower concentrations of fresh biogenic OC due to its post-depositional degradation. Hence, it is probable that different sampling techniques might have, at least partly, contributed the difference between the site SS4 in 1987 and the site ARA05C-34BC collected in 2014. However, comparable data are limited to draw irrefutable conclusions at present. Therefore, our hypothesis that accelerated permafrost thawing in response to recent Arctic warming enhanced land–ocean OC transfer should be further explored through the down-core analyses of well dated sediment cores, as our current results are based on snapshot data.

We further separated the biogenic OC to soil-derived, plant-derived, and marine OC, by applying a three end-member mixing model based on $\delta^{13}C_{org}$ and 3,5-Bd/V values (cf. Smith et al., 2015). Due to significant contributions of petrogenic OC to the Beaufort Sea, we corrected the isotopic signature of petrogenic OC from the measured $\delta^{13}C_{org}$ values as follows (cf. Smith et al., 2015):

$$\delta^{13}C_{org-measured} = \delta^{13}C_{petro} * f_{petro} + \delta^{13}C_{org-corrected} * f_{bio} \quad (6)$$

$$f_{petro} + f_{bio} = 1 \quad (7)$$

where $\delta^{13}C_{org\text{-}measured}$ is the observed $\delta^{13}C_{org}$ value of the sediment sample, $\delta^{13}C_{petro}$ is the average $\delta^{13}C$ of OC_{petro} in the Arctic rivers of −27.6 ± 2.7‰ (n = 58, Goñi et al., 2005; Schwab et al., 2021 and references therein), $\delta^{13}C_{org\text{-}corrected}$ is the average of biogenic OC $\delta^{13}C$ values, and f_{petro} and f_{bio} represent the OC fraction composed of petrogenic and biogenic organic constituents. We used the data for f_{petro} and f_{bio} obtained from Method 3 (cf. Vonk et al., 2015) rather than Method 2 (cf. Galy et al., 2008), since the former appears to better represent the hydrodynamic sorting effect (see Fig. S4). Based on the $\delta^{13}C_{org\text{-}corrected}$ and 3,5-Bd/V values (see Table S4), we calculated the relative contributions of soil-derived, plant-derived, and marine OC to the biogenic OC, by applying the "IsoSource" model (version 1.3.1, http://www.epa.gov/wed/pages/models/stableIsotopes/iso-source/isosource.htm). The source increment and mass balance tolerance values were of 1% and 0.1‰, respectively. The $\delta^{13}C_{org}$ and 3,5-Bd/V values used as the end-members (Fig. 10) were −26.3 ± 0.4‰ (n = 24) and 0.65 (n = 1) for soils (Schreiner et al., 2013; Bröder et al., 2021), −30.7‰ (n = 1) and 0.03 ± 0.03 (n = 12) for vascular plants (Moingt et al., 2016), and −20.2 ± 1.70‰ (n = 2) and 0.00 (n = 2) for marine OC (Goñi et al., 2000). Note that Al data were unavailable for the samples from the Mackenzie Shelf which hampered the application of the three end-member mixing model for the biogenic OC fraction. The soil-derived OC fractions increased from 9.7% to 19.6% with water depth, while the petrogenic OC fractons showed similar values between 37% and 41% (Fig. 11). The average soil-derived OC contribution to sedimentary OC was lower in the Mackenzie Trough (14.5 ± 4.0%) than in the Beaufort slope (22.2 ± 2.2%) (Fig. S5). The plant-derived OC proportions decreased with distance offshore (Fig. 11), with higher values in the Mackenzie Trough (17.6 ± 4.8%) than those in the Beaufort slope (6.6 ± 2.7%) (Fig. S5). In contrast, the contributions of marine OC increased with water depth

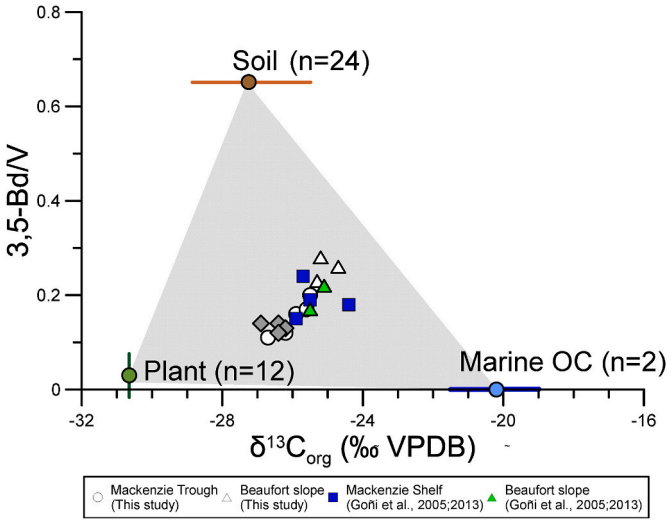

Fig. 10. Scatter plot of $\delta^{13}C_{org}$ (‰ VPDB) vs. 3,5-Bd/V to constrain biogenic OC sources. The three end-member values were compiled from the literature for soils (Schreiner et al., 2013; Bröder et al., 2021), vascular plants (Moingt et al., 2016), and marine OC (Goñi et al., 2000).

(Fig. 11). Thus, the marine OC contribution to sedimentary OC was slightly higher in the Beaufort slope (29.6 ± 3.9%) than in the Mackenzie Trough (28.7 ± 2.0%) (Fig. 11, see also Fig. S5). Unfortunately, comparable lignin data for the SS4 sample were unavailable which prevented us to compare the results from the four end-member approach between the site SS4 in 1987 and the site ARA05C-34BC collected in 2014. Our results from the four end-member approach suggest that the increasing $\Delta^{14}C_{org}$ values along the Mackenzie Trough were strongly governed by the enrichment of marine OC superimposed by the effect of the increased contribution of soil-derived OC to sedimentary OC, probably due to the degradation of more fresher vascular plant material (Fig. 11). Previously, Drenzek et al. (2007) assessed the relative contributions of aged soil-derived terrestrial OC apart from the petrogenic and marine OC on the Mackenzie Shelf based on the $\delta^{13}C$ and $\Delta^{14}C$ signatures of individual extractable *n*-fatty acids and alkanes in addition to those of pyrolysate alkanes. Similarly, our approach combining bulk and molecular markers can be a valuable tool to decern the relative contributions of fresher vascular plant-derived, pre-aged soil-derived, and marine OC to biogenic OC apart from the petrogenic OC contribution to sedimentary OC and thus to better assess the land-ocean OC transfer and the fate of permafrost-derived OC in the rapidly changing Canadian Arctic.

5. Conclusions

In this study, we applied inorganic and organic geochemical techniques as well as sedimentological measurements to investigate surface sediment samples collected along a Mackenzie Trough transect in the Canadian Beaufort Sea. We found that hydrodynamic sorting of particles decreased the OC loading at deeper water depths. In addition, OC loading was further influenced by the increased degradation of terrestrial OC and the increased contribution of marine OC with distance offshore. The estimated BE of terrestrial OC was higher in the Mackenzie Trough than in the Beaufort slope. In contrast, the estimates of the ^{14}C composition of the biogenic OC fraction (i.e., Fm_{bio}) were lower in the Mackenzie Trough than in the Beaufort slope. We were unable to adequately compare our estimates from the Canadian Beaufort Sea with those previously published due to the limited data coverage. Hence, further investigations using long-term sediment core records are necessary to fully elucidate the mobilization and fate of permafrost-derived OC in the rapidly changing Canadian Arctic.

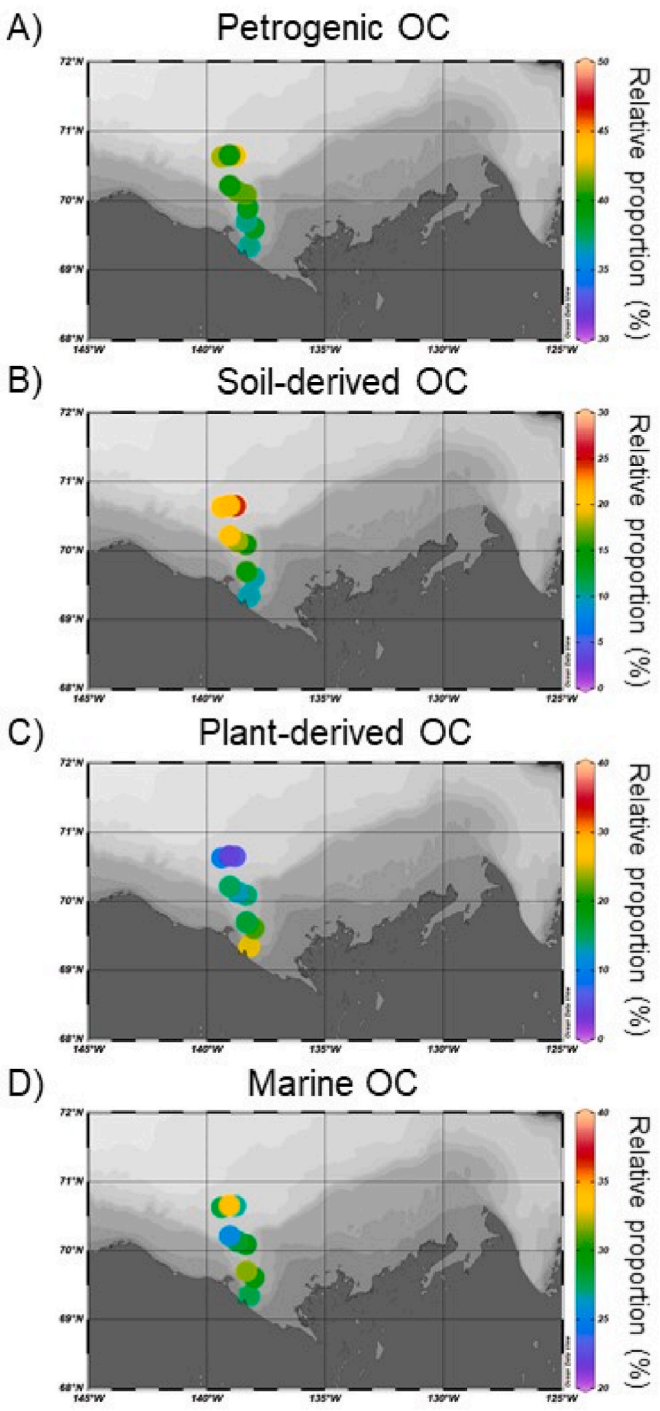

Fig. 11. Spatial variations of the petrogenic and biogenic (i.e., soil-derived, plant-derived, and marine) OC fractions obtained from the combined approaches by Vonk et al. (2015) and Smith et al. (2015).

CRediT authorship contribution statement

Dahae Kim: Writing – review & editing, Writing – original draft, Visualization, Methodology, Data curation, Conceptualization. **Jung-Hyun Kim:** Writing – review & editing, Writing – original draft, Visualization, Supervision, Project administration, Methodology, Data curation, Conceptualization. **Tommaso Tesi:** Writing – review & editing, Methodology, Data curation. **Sujin Kang:** Methodology, Data curation. **Alessio Nogarotto:** Methodology. **Kwangkyu Park:** Investigation. **Dong-Hun Lee:** Investigation. **Young Keun Jin:** Investigation,

Funding acquisition. **Kyung-Hoon Shin:** Methodology. **Seung-Il Nam:** Writing – review & editing, Methodology, Investigation, Funding acquisition.

Declaration of competing interest

The authors declare that they have no known competing financial interests or personal relationships that could have appeared to influence the work reported in this paper.

Data availability

Data will be made available on request.

Acknowledgments

We thank two anonymous reviewers for their insightful comments that greatly improved the quality of our manuscript. We acknowledge the captain and crew of R/V *Araon* for their support at sea with sediment core retrievals. We also thank Y. Son and Y. Joe for their analytical and graphical assistance in the laboratory at KOPRI. This study was supported by the Korea Institute of Marine Science and Technology Promotion (KIMST Grant 20210632; KOPRI-PM22050) funded by the Ministry of Oceans and Fisheries and the National Research Foundation of Korea (NRF) grant funded through the Ministry of Science and ICT (NRF-2021M1A5A1075512; KOPRI-PN22013).

Appendix A. Supplementary data

Supplementary data to this article can be found online at https://doi.org/10.1016/j.ecss.2022.107997.

References

Aller, R.C., Blair, N.E., 2006. Carbon remineralization in the Amazon–Guianas tropical mobile mudbelt: a sedimentary incinerator. Continent. Shelf Res. 26, 2241–2259. https://doi.org/10.1016/j.csr.2006.07.016.

Barnhart, K.R., Anderson, R.S., Overeem, I., Wobus, C., Clow, G.D., Urban, F.E., 2014. Modeling erosion of ice-rich permafrost bluffs along the Alaskan Beaufort Sea coast. J. Geophys. Res. Earth Surf. 119, 1155–1179. https://doi.org/10.1002/2013JF002845.

Belika, L.L., Macdonald, R.W., Yunker, M.B., Harvey, H.R., 2004. The role of depositional regime on carbon transport and preservation in Arctic Ocean sediments. Mar. Chem. 86, 65–88. https://doi.org/10.1016/j.marchem.2003.12.006.

Blair, N.E., Aller, R.C., 2012. The fate of terrestrial organic carbon in the marine environment. Ann. Rev. Mar. Sci 4, 401–423. https://doi.org/10.1146/annurev-marine-120709-142717.

Blasco, S.M., Fortin, G., Hill, P.R., O'Connor, M.J., Brigham-Grette, J.K., 1990. The late Neogene and Quaternary stratigraphy of the Canadian Beaufort continental shelf. In: Grantz, A., Johnson, L., Sweeney, J.F. (Eds.), The Arctic Ocean Region. The Geology of North America, pp. 491–502. https://doi.org/10.1130/DNAG-GNA-L.491.

Bray, E.E., Evans, E.D., 1961. Distribution of *n*-paraffins as a clue to recognition of source beds. Geochem. Cosmochim. Acta 22, 2–15. https://doi.org/10.1016/0016-7037(61)90069-2.

Bröder, L., Tesi, T., Salvadó, J.A., Semiletov, I.P., Dudarev, O.V., Gustafsson, Ö., 2016. Fate of terrigenous organic matter across the Laptev Sea from the mouth of the Lena River to the deep sea of the Arctic interior. Biogeosciences 13, 5003–5019. https://doi.org/10.5194/bg-13-5003-2016.

Bröder, L., Keskitalo, K., Zolkos, S., Shakil, S., Tank, S., Kokelj, S., Tesi, T., Dongen, B.V., Haghipour, N., Eglinton, T.I., Vonk, J.E., 2021. Preferential export of permafrost-derived organic matter as retrogressive thaw slumping intensifies. Environ. Res. Lett. 16, 054059 https://doi.org/10.1088/1748-9326/abee4b.

Buggle, B., Wiesenberg, G.L.B., Glaser, B., 2010. Is there a possibility to correct fossil *n*-alkane data for postsedimentary alteration effects? Appl. Geochem. 25, 947–957. https://doi.org/10.1016/j.apgeochem.2010.04.003.

Carmack, E.C., Macdonald, R.W., 2002. Oceanography of the Canadian shelf of the Beaufort Sea: a setting for marine life. Arctic 55, 29–45. https://doi.org/10.14430/arctic733.

Cranwell, P.A., 1981. Diagenesis of free and bound lipids in terrestrial detritus deposited in a lacustrine sediment. Org. Geochem. 3, 79–89. https://doi.org/10.1016/0146-6380(81)90002-4.

Cranwell, P.A., Eglinton, G., Robinson, N., 1987. Lipids of aquatic organisms as potential contributors to lacustrine sediments–II. Org. Geochem. 11, 513–527. https://doi.org/10.1016/0146-6380(87)90007-6.

Derrien, M., Cabrera, F.A., Tavera, N.L.V., Manzano, C.A.K., Vizcaino, S.C., 2015. Sources and distribution of organic matter along the Ring of Cenotes, Yucatan, Mexico: sterol markers and statistical approaches. Sci. Total Environ. 511, 223–229. https://doi.org/10.1016/j.scitotenv.2014.12.053.

Dellinger, M., Gaillardet, J., Bouchez, J., Calmels, D., Galy, V., Hilton, R.G., Louvat, P., France-Lanord, C., 2014. Lithium isotopes in large rivers reveal the cannibalistic nature of modern continental weathering and erosion. Earth Planet Sci. Lett. 410, 359–372. https://doi.org/10.1016/j.epsl.2014.05.061.

Druffel, E.R.M., Griffin, S., Glynn, C.S., Benner, R., Walker, B.D., 2017. Radiocarbon in dissolved organic and inorganic carbon of the Arctic Ocean. Geophys. Res. Lett. 44, 2369–2376. https://doi.org/10.1002/2016GL072138.

Dickens, A.F., Gudeman, J.A., Gélinas, Y., Baldock, J.A., Tinner, W., Hu, F.S., Hedges, J. I., 2007. Sources and distribution of CuO derived benzene carboxylic acids in soils and sediments. Org. Geochem. 38, 1256–1276. https://doi.org/10.1016/j.orggeochem.2007.04.004.

Ding, L., Zhao, M., Yu, M., Li, L., Huang, C.-Y., 2017. Biomarker assessments of sources and environmental implications of organic matter in sediments from potential cold seep areas of the northeastern South China Sea. Acta Oceanol. Sin. 36, 8–19. https://doi.org/10.1007/s13131-017-1068-1.

Drenzek, N., Montlucon, D.B., Yunker, M.B., Macdonald, R.W., Eglinton, T.I., 2007. Constraints on the origin of sedimentary organic carbon in the Beaufort Sea from coupled molecular ^{13}C and ^{14}C measurements. Mar. Chem. 103, 146–162. https://doi.org/10.1016/j.marchem.2006.06.017.

Eglinton, G., Hamilton, R.J., 1967. Leaf epicuticular waxes. Science 156, 1322–1335.

Eglinton, T.I., Galy, V.V., Hemingway, J.D., Feng, X., Bao, H., Blattmann, T.M., 2021. Climate control on terrestrial biospheric carbon turnover. Proc. Natl. Acad. Sci. USA 118, e2011585118. https://doi.org/10.1073/pnas.2011585118.

Ertel, J.R., Hedges, J.I., Devol, A.H., Richey, J.E., Ribeiro, M., 1986. Dissolved humic substances in the Amazon River system. Limnol. Oceanogr. 31, 739–754. https://doi.org/10.4319/lo.1986.31.4.0739.

Friedlingstein, P., Jones, M.W., O'Sullivan, M., Andrew, R.M., Hauck, J., Peters, G.P., Peters, W., Pongratz, J., Sitch, S., Quéré, C.L., Bakker, D.C.E., Canadell, J.G., Ciais, P., Jackson, R.B., Anthoni, P., Barbero, L., Bastos, A., Bastrikov, V., Becker, M., Bopp, L., Buitenhuis, E., Chandra, N., Chevallier, F., Chini, L.P., Currie, K.I., Feely, R. A., Gehlen, M., Gilfillan, D., Gkritzalis, T., Goll, D.S., Gruber, N., Gutekunst, S., Harris, I., Haverd, V., Houghton, R.A., Hurtt, G., Ilyina, T., Jain, A.K., Joetzjer, E., Kaplan, J.O., Kato, E., Goldewijk, K.K., Korsbakken, J.I., Landschützer, P., Lauvset, S. K., Lefèvre, N., Lenton, A., Lienert, S., Lombardozzi, D., Marland, G., McGuire, P.C., Melton, J.R., Metzl, N., Munro, D.R., Nabel, J.E.M.S., Nakaoka, S.-I., Neill, C., Omar, A.M., Ono, T., Peregon, A., Pierrot, D., Poulter, B., Rehder, G., Resplandy, L., Robertson, E., Rödenbeck, C., Séférian, R., Schwinger, J., Smith, N., Tans, P.P., Tian, H., Tilbrook, B., Tubiello, F.N., van der Werf, G.R., Wiltshire, A.J., Zaehle, S., 2019. Global carbon budget 2019. Earth Syst. Sci. Data 11, 1783–1838. https://doi.org/10.5194/essd-11-1783-2019.

Galy, V., Beyssack, O., France-Lanord, C., Eglinton, T., 2008. Recycling of graphite during Himalayan erosion: a geological stabilization of carbon in the crust. Science 322, 943–945. http://doi:10.1126/science.1161408.

Goñi, M.A., Hedges, J.I., 1990. Potential applications of cutin-derived Cuo reaction products for discriminating vascular plant tissues in natural environments. Geochem. Cosmochim. Acta 54, 3073–3081. https://doi.org/10.1016/0016-7037(90)90123-3.

Goñi, M.A., Hedges, J.I., 1992. Lignin dimers: structures, distribution, and potential geochemical applications. Geochem. Cosmochim. Acta 56, 4025–4043. https://doi.org/10.1016/0016-7037(92)90014-A.

Goñi, M.A., Hedges, J.I., 1995. Sources and reactivities of marine-derived organic matter in coastal sediments as determined by alkaline CuO oxidation. Geochem. Cosmochim. Acta 59, 2965–2981. https://doi.org/10.1016/0016-7037(95)00188-3.

Goñi, M.A., Yunker, M.B., MacDonald, R.W., Eglinton, T.I., 2000. Distribution and sources of organic biomarkers in arctic sediments from the Mackenzie River and Beaufort Shelf. Mar. Chem. 71, 23–51. https://doi.org/10.1016/S0304-4203(00)00037-2.

Goñi, M.A., Yunker, M.B., MacDonald, R.W., Eglinton, T.I., 2005. The supply and preservation of ancient and modern components of organic carbon in the Canadian Beaufort Shelf of the Arctic Ocean. Mar. Chem. 93, 53–73. https://doi.org/10.1016/j.marchem.2004.08.001.

Goñi, M.A., O'Connor, A.E., Kuzyk, Z.Z., Yunker, M.B., Gobeil, C., Macdonald, R.W., 2013. Distribution and sources of organic matter in surface marine sediments across the North American Arctic margin. J. Geophys. Res. Oceans 118, 4017–4035. https://doi.org/10.1002/jgrc.20286.

Griffith, D.R., McNichol, A.P., Xu, L., McLaughlin, F.A., Macdonald, R.W., Brown, K.A., Eglinton, T.I., 2012. Carbon dynamics in the western Arctic Ocean: insights from full-depth carbon isotope profiles of DIC, DOC, and POC. Biogeosciences 9, 1217–1224. https://doi.org/10.5194/bgd-8-10677-2011.

Grosse, G., Goetz, S., McGuire, A.D., Romanovsky, V.E., Schuur, E.A.G., 2016. Changing permafrost in a warming world and feedbacks to the Earth system. Environ. Res. Lett. 11, 040201 https://doi.org/10.1088/1748-9326/11/4/040201.

Gustafsson, Ö., van Dongen, B.E., Vonk, J.E., Dudarev, O.V., Semiletov, I.P., 2011. Widespread release of old carbon across the Siberian Arctic echoed by its large rivers. Biogeosciences 8, 1737–1743. https://doi.org/10.5194/bg-8-1737-2011.

Haine, T.W.N., Curry, B., Gerdes, R., Hansen, E., Karcher, M., Lee, C., Rudels, B., Spreen, G., de Steur, L., Stewart, K.D., Rebecca, W., 2015. Arctic freshwater export: status, mechanisms, and prospects. Global Planet. Change 125, 13–35. https://doi.org/10.1016/j.gloplacha.2014.11.013.

Han, J., Calvin, M., 1969. Hydrocarbon distribution of algae and bacteria, and microbiological activity in sediments. Proc. Natl. Acad. Sci. USA 64, 436–443. https://doi.org/10.1073/pnas.64.2.436.

Hartnett, H.E., Keil, R.G., Hedges, J.I., Devol, A.H., 1998. Influence of oxygen exposure time on organic carbon preservation in continental margin sediments. Nature 391, 572–574. https://doi.org/10.1038/35351.

Hedges, J.I., Ertel, J.R., 1982. Characterization of lignin by gas capillary chromatography of cupric oxide oxidation products. Anal. Chem. 54, 174–178. https://doi.org/10.1021/ac00239a007.

Hedges, J.I., Hu, F.S., Devol, A.H., Hartnet, H.E., Tsamakis, E., Keil, R.G., 1999. Sedimentary organic matter preservation: a test for selective degradation under oxic conditions. Am. J. Sci. 299, 529–555. https://doi.org/10.2475/ajs.299.7-9.529.

Hedges, J.I., Mann, D.C., 1979. The characterization of plant tissues by their lignin oxidation products. Geochem. Cosmochim. Acta 43, 1803–1807. https://doi.org/10.1016/0016-7037(79)90028-0.

Houel, S., Louchouarn, P., Lucotte, M., Canuel, R., Ghaleb, B., 2006. Translocation of soil organic matter following reservoir impoundment in boreal systems: implications for in situ productivity. Limnol. Oceanogr. 51, 1497–1513. https://doi.org/10.4319/lo.2006.51.3.1497.

Hill, P.R., Blasco, S.M., Harper, J.R., Fissel, D.B., 1991. Sedimentation on the Canadian Beaufort shelf. Continent. Shelf Res. 11, 821–842. https://doi.org/10.1016/0278-4343(91)90081-G.

Hilton, R.G., Galy, A., Hovius, N., Horng, M.J., Chen, H., 2010. The isotopic composition of particulate organic carbon in mountain rivers of Taiwan. Geochem. Cosmochim. Acta 74, 3164–3181. https://doi.org/10.1016/j.gca.2010.03.004.

Hilton, R.G., Galy, V., Gaillardet, J., Dellinger, M., Bryant, C., O'Regan, M., Grocke, D.R., Coxall, H., Bouchez, J., Calmels, D., 2015. Erosion of organic carbon in the Arctic as a geological carbon dioxide sink. Nature 524, 84–88. https://doi.org/10.1038/nature14653.

Huang, W.Y., Meinschein, W.G., 1976. Sterols as source indicators of organic material in sediments. Geochem. Cosmochim. Acta 40, 323–330. https://doi.org/10.1016/0016-7037(76)90210-6.

Huang, Y., Bol, R., Harkness, D.D., Ineson, P., Eglinton, G., 1996. Post-glacial variations in distributions, ^{13}C and ^{14}C contents of aliphatic hydrocarbons and bulk organic matter in three types of British acid upland soils. Org. Geochem. 24, 273–287. https://doi.org/10.1016/0146-6380(96)00039-3.

Hugelius, G., Strauss, J., Zubrzycki, S., Harden, J.W., Schuur, E.A.G., Ping, C.-L., Schirrmeister, L., Grosse, G., Michaelson, G.J., Koven, C.D., O'Donnell, J.A., Elberling, B., Mishra, U., Camill, P., Yu, Z., Palmtag, J., Kuhry, P., 2014. Estimated stocks of circumpolar permafrost carbon with quantified uncertainty ranges and identified data gaps. Biogeosciences 11, 6573–6593. https://doi.org/10.5194/bg-11-6573-2014.

IPCC, 2013. Climate change 2013: the physical science basis. In: Stocker, T.F., Qin, D., Plattner, G.-K., Tignor, M., Allen, S.K., Boschung, J., Nauels, A., Xia, Y., Bex, V., Midgley, P.M. (Eds.), Contribution of Working Group I to the Fifth Assessment Report of the Intergovernmental Panel on Climate Change. Cambridge University Press, Cambridge, UK and New York, NY, USA. https://doi.org/10.1017/CBO9781107415324, 1535 pp.

ISO 9277, 2010. Determination of the Specific Surface Area of Solids by Gas Adsorption – BET Method. http://iso.org/standard/44941.html.

Joo, Y., Forwick, M., Park, K., Joe, Y., Son, Y., Nam, S.-I., 2019. Holocene environmental changes in Dicksonfjorden, west Spitsbergen, Svalbard. Polar Res. 38, 3426–3439. https://doi.org/10.33265/polar.v38.3426.

Keil, R.G., Dickens, A.F., Arnarson, T., Nunn, B.L., Devol, A.H., 2004. What is the oxygen exposure time of laterally transported organic matter along the Washington margin? Mar. Chem. 92, 157–165. https://doi.org/10.1016/j.marchem.2004.06.024.

Keil, R.G., Tsamakis, E., Fuh, C.B., Giddings, J.C., Hedges, J.I., 1994. Mineralogical and textural controls on the organic composition of coastal marine sediments: hydrodynamic separation using SPLITT-fractionation. Geochem. Cosmochim. Acta 58, 879–893. https://doi.org/10.1016/0016-7037(94)90512-6.

Keil, R.G., Tsamakis, E., Giddings, J.C., Hedges, J.I., 1998. Biochemical distributions (amino acids, neutral sugars, and lignin phenols) among size-classes of modern sediments from the Washington coast. Geochem. Cosmochim. Acta 62, 1347–1364. https://doi.org/10.1016/S0016-7037(98)00080-5.

Keil, R.G., Mayer, L.M., Quay, P.D., Richey, J.E., Hedges, J.I., 1997. Loss of organic matter from riverine particles in deltas. Geochem. Cosmochim. Acta 61, 1507–1511. https://doi.org/10.1016/S0016-7037(97)00044-6.

Kim, D., Kim, J.-H., Kim, M.-S., Ra, K., Shin, K.-H., 2018. Assessing environmental changes in Lake Shihwa, South Korea, based on distributions and stable carbon isotopic compositions of *n*-alkanes. Environ. Pollut. 240, 105–115. https://doi.org/10.1016/j.envpol.2018/04.098.

Kim, J.-H., Gal, J.-K., Jun, S.-Y., Smik, L., Kim, D., Belt, S.T., Park, K., Shin, K.-H., Nam, S.-I., 2019. Reconstructing spring sea ice concentration in the Chukchi Sea over recent centuries: insights into the application of the PIP_{25} index. Environ. Res. Lett. 14 https://doi.org/10.1088/1748-9326/ab4b6e.

Knies, J., Brookes, S., Schubert, C.J., 2007. Re-assessing the nitrogen signal in continental margin sediments: new insights from the high northern latitudes. Earth Planet Sci. Lett. 253, 471–484. https://doi.org/10.1016/j.epsl.2006.11.008.

Louchouarn, P., Lucotte, M., Farella, N., 1999. Historical and geographical variations of sources and transport of terrigenous organic matter within a large-scale coastal environment. Org. Geochem. 30, 675–699. https://doi.org/10.1016/S0146-6380(99)00019-4.

Macdonald, R.W., Solomon, S.M., Cranston, R.E., Welch, H.E., Yunker, M.B., Gobeil, C., 1998. A sediment and organic carbon budget for the Canadian Beaufort Shelf. Mar. Geol. 144, 255–273. https://doi.org/10.1016/S0025-3227(97)00106-0.

Magen, C., Chaillou, G., Crowe, S.A., Mucci, A., Sundby, B., Gao, A., Makabe, R., Sasake, H., 2010. Origin and fate of particulate organic matter in the southern Beaufort Sea – Amundsen Gulf region, Canadian Arctic. Estuar. Coast Shelf Sci. 86, 31–41. https://doi.org/10.1016/j.ecss.2009.09.009.

Mann, P.J., Strauss, J., Palmtag, J., Dowdy, K., Ogneva, O., Fuchs, M., Bedington, M., Torres, R., Polimene, L., Overduin, P., Mollenhauer, G., Grosse, G., Rachold, V., Sobczak, W.V., Spencer, R.G.M., Juhls, B., 2022. Degrading permafrost river catchments and their impact on Arctic Ocean nearshore processes. Ambio 51, 439–455. https://doi.org/10.1007/s13280-021-01666-z.

Mayer, L.M., 1994. Surface area control of organic carbon accumulation in continental shelf sediments. Geochem. Cosmochim. Acta 58, 1271–1284. https://doi.org/10.1016/0016-7037(94)90381-6.

McClelland, J.W., 2016. Particulate organic carbon and nitrogen export from major Arctic rivers. Global Biogeochem. Cycles 30, 629–643. https://doi.org/10.1002/2015GB005351.

McMahon, R., Taveras, Z., Neubert, P., Harvey, H.R., 2021. Organic biomarkers and Meiofauna diversity reflect distinct carbon sources to sediments transecting the Mackenzie continental shelf. Continent. Shelf Res. 2021, 104406 https://doi.org/10.1016/j.csr.2021.104406.

Meile, C., van Cappellen, P., 2005. Particle age distributions and O2 exposure times: timescales in bioturbated sediments. Global Biogeochem. Cycles 19, GB3013. https://doi.org/10.1029/2004GB002371.

Meyers, P.A., Ishlwatari, R., 1993. The early diagenesis of organic matter in lacustrine sediments. In: Engel, M., Macko, S.A. (Eds.), Organic Geochemistry. Plenum, New York, pp. 185–209. https://doi.org/10.1007/978-1-4615-2890-6_8.

Moingt, M., Lucotte, M., Paquet, S., 2016. Lignin biomarkers signatures of common plants and soils of Eastern Canada. Biogeochemistry 129, 133–148. https://doi.org/10.1007/s10533-016-0223-7.

Naidu, A.S., Cooper, L.W., Finney, B.P., Macdonald, R.W., Alexander, C., Semiletov, I.P., 2000. Organic carbon isotope ratios ($\delta^{13}C$) of Arctic Amerasian continental shelf sediments. Int. J. Earth Sci. 89, 522–532. https://doi.org/10.1007/s005310000121.

O'brien, M., Macdonald, R.W., Melling, H., Iseki, K., 2006. Particle fluxes and geochemistry on the Canadian Beaufort Shelf: implications for sediment transport and deposition. Continent. Shelf Res. 26, 41–81. https://doi.org/10.1016/j.csr.2005.09.007.

Opsahl, S., Benner, R., 1995. Early diagenesis of vascular plant tissues: lignin and cutin decomposition and biogeochemical implications. Geochem. Cosmochim. Acta 59, 4889–4904. http://doi:10.1016/0016-7037(95)00348-7.

Otto, A., Simpson, M.J., 2006. Evaluation of CuO oxidation parameters for determining the source and stage of lignin degradation in soil. Biogeochemistry 80, 121–142. https://doi.org/10.1007/s10533-006-9014-x.

Prahl, F.G., Ertel, J.R., Goñi, M.A., Sparrow, M.A., Eversmeyer, B., 1994. Terrestrial organic carbon contributions to sediments on the Washington margin. Geochem. Cosmochim. Acta 58, 3035–3048. https://doi.org/10.1016/0016-7037(94)90177-5.

Rampton, V.N., 1982. Quaternary geology of the Yukon coastal plain. Geol. Surv. Can. Bull. 317 https://doi.org/10.4095/111347, 49 pp.

Sánchez-García, L., Alling, V., Pugach, S., Vonk, J., van Dongen, B., Humborg, C., Dudarev, O., Semiletov, I., Gustafsson1, Ö., 2011. Inventories and behavior of particulate organic carbon in the Laptev and East Siberian seas. Global Biogeochem. Cycles 25, GB2007. https://doi.org/10.1029/2010GB003862.

Schreiner, K.M., Bianchi, T.S., Eglinton, T.I., Allison, M.A., Hanna, A.J.M., 2013. Sources of terrigenous inputs to surface sediments of the Colville River delta and Simpson's Lagoon, Beaufrot sea, Alaska. J. Geophys. Res. 118, 808–824. https://doi.org/10.1002/jgrg.20065.

Schwab, M.S., Rickli, J.D., Macdonald, R.W., Harvey, H.R., Haghipour, N., Eglinton, T.I., 2021. Detrital neodymium and (radio)carbon as complementary sedimentary bedfellows? The Western Arctic Ocean as a testbed. Geochem. Cosmochim. Acta 315, 101–126. https://doi.org/10.1016/j.gca.2021.08.019.

Schubert, C.J., Calvert, S.E., 2001. Nitrogen and carbon isotopic composition of marine and terrestrial organic matter in Arctic Ocean sediments. Deep-Sea Res. 48, 789–810. https://doi.org/10.1016/S0967-0637(00)00069-8.

Schurr, E.A.G., McGuire, A.D., Schädel, C., Grosse, G., Harden, J.W., Hayes, D.J., Hugelius, G., Koven, C.D., Kuhry, P., Lawrence, D.M., Natali, S.M., Olefeldt, D., Romanovsky, V.E., Schaefer, K., Turetsky, M.R., Treat, C.C., Vonk, J.E., 2015. Climate change and the permafrost carbon feedback. Nature 520, 171–179. https://doi.org/10.1038/nature14338.

Semiletov, I., Pipko, I., Gustafsson, Ö., Anderson, L.G., Sergienko, V., Pugach, S., Dudarev, O., Charkin, A., Gukov, A., Bröder, L., Andersson, A., Spivak, E., Shakhova, N., 2016. Acidification of East Siberian Arctic Shelf waters through addition of freshwater and terrestrial carbon. Nat. Geosci. 9, 361–365. https://doi.org/10.1038/ngeo2695.

Shearer, J.M., 1971. Preliminary interpretation of shallow seismic reflection profiles from the west side of Mackenzie Bay, Beaufort Sea. Report of Activities. Part B, Geol. Surv. Can. 71–1, 131–138. https://doi.org/10.4095/105499.

Silva, J.A., Bremner, J.M., 1966. Determination and isotope ratio analysis of different forms of nitrogen in soils. 5. Fixed ammonium. Soil Sci. Soc. Am. Proc. 30, 587–594. https://doi.org/10.2136/sssaj1966.03615995003000050017x.

Smith, W.R., Bianchi, T., Allison, M., Savage, C., Galy, V., 2015. High rates of organic carbon burial in fjord sediments globally. Nat. Geosci. 8, 450–453. http://doi/org/10.1038/ngeo2421.

Stein, R., MacDonald, R.W., 2004. The Organic Carbon Cycle in the Arctic Ocean. Springer–Verlag, New York. https://doi.org/10.1007/978-3-642-18912-8_2, 400 pp.

Stuiver, M., Braziunas, T.F., 1993. Modeling atmospheric ^{14}C influences and ^{14}C ages of marine samples to 10,000 BC. Radiocarbon 35, 137–189. https://doi.org/10.1017/S0033822200013874.

Tarnocai, C., Canadell, J.G., Schuur, E.A.G., Kuhry, P., Mazhitova, G., Zimov, S., 2009. Soil organic carbon pools in the northern circumpolar permafrost region. Global Biogeochem. Cycles 23, GB2023. https://doi.org/10.1029/2008GB003327.

Tesi, T., Semiletov, I., Hugelius, G., Dudarev, O., Kuhry, P., Gustafsson, Ö., 2014. Composition and fate of terrigenous organic matter along the Arctic land–ocean continuum in East Siberia: insights from biomarkers and carbon isotopes. Geochem. Cosmochim. Acta 133, 235–256. https://doi.org/10.1016/j.gca.2014.02.045.

Volkman, J.K., 1986. A review of sterol markers for marine and terrigenous organic matter. Org. Geochem. 9, 83–99. https://doi.org/10.1016/0146-6380(86)90089-6.

Vonk, J.E., Gustafsson, Ö., 2013. Permafrost-carbon complexities. Nat. Geosci. 6, 675–676. https://doi.org/10.1038/ngeo1937.

Vonk, J.E., Giosan, L., Blusztajn, J., Montlucon, D., Pannatier, E.G., McIntyre, C., Wacker, L., Macdonald, R.W., Yunker, M.B., Eglinton, T.I., 2015. Spatial variations in geochemical characteristics of the modern Mackenzie Delta sedimentary system. Geochem. Cosmochim. Acta 171, 100–120. https://doi.org/10.1016/j.gca.2015.08.005.

Yunker, M.B., Backus, S.M., Pannatier, E.G., Jeffries, D.S., Macdonald, R.W., 2002. Sources and significance of alkane and PAH hydrocarbons in Canadian Arctic Rivers. Estuar. Coast Shelf Sci. 55, 1–31. https://doi.org/10.1006/ecss.2001.0880.

Yunker, M.B., Belicka, L.L., Harvey, H.R., Macdonald, R.W., 2005. Tracing the inputs and fate of marine and terrigenous organic matter in Arctic Ocean sediments: a multivariate analysis of lipid biomarkers. Deep-Sea Res. 52, 3478–3508. https://doi.org/10.1016/j.dsr2.2005.09.008.

Yunker, M.B., Macdonald, R.W., Fowler, B.R., Cretney, W.J., Dallimore, S.R., Mclaughlin, F.A., 1990. Geochemistry and fluxes of hydrocarbons to the Beaufort Sea shelf: a multivariate comparison of fluvial inputs and coastal erosion of peat using principal components analysis. Geochem. Cosmochim. Acta 55, 255–273. https://doi.org/10.1016/0016-7037(91)90416-3.

Yunker, M.B., Macdonald, R.W., Snowdon, L.R., Fowler, B.R., 2011. Alkane and PAH biomarkers as tracers of terrigenous organic carbon in Arctic Ocean sediments. Org. Geochem. 42, 1109–1146. https://doi.org/10.1016/j.orggeochem.2011.06.007.

Yunker, M.B., Macdonald, R.W., Veltkamp, D.J., Cretney, W.J., 1995. Terrestrial and marine biomarkers in a seasonally ice-covered Arctic estuary - integration of multivariate and biomarker approaches. Mar. Chem. 49, 1–50. https://doi.org/10.1016/0304-4203(94)00057-K.

Zhang, T., Barry, R.G., Knowles, K., Heginbottom, J.A., Brown, J., 1999. Statistics and characteristics of permafrost and ground-ice distribution in the Northern Hemisphere. Polar Geogr. 23, 132–154. https://doi.org/10.1080/10889370802175895.